Manuscript prepared for Atmos. Chem. Phys. Discuss.
with version 2014/07/09 7.01 Copernicus papers of the LaTeX class copernicus.cls.
Date: 29 April 2015

Seasonal variability of atmospheric nitrogen oxides and non-methane hydrocarbons at the GEOSummit station, Greenland

L. J. Kramer[1], D. Helmig[2], J. F. Burkhart[3,4], A. Stohl[5], S. Oltmans[6,7], and R. E. Honrath[1,†]

[1]Atmospheric Sciences Program/Dept. of Geological and Mining Engineering and Sciences, Michigan Technological University, Houghton, Michigan, USA
[2]Institute of Arctic and Alpine Research, University of Colorado, Boulder, CO, USA
[3]Department of Geosciences, University of Oslo, Norway
[4]Sierra Nevada Research Institute, University of California, Merced, USA
[5]Norwegian Institute for Air Research (NILU), Kjeller, Norway
[6]NOAA Earth System Research Laboratory, Boulder, CO, USA
[7]CIRES, University of Colorado, Boulder, Colorado, USA
[†]deceased

Correspondence to: L. J. Kramer (lkramer@mtu.edu)

Abstract

Measurements of atmospheric nitrogen oxides NO_x ($NO_x = NO + NO_2$), peroxyacetyl nitrate (PAN), NO_y, and non-methane hydrocarbons (NMHC) were taken at the GEOSummit Station, Greenland (72.34° N, 38.29° W, 3212 m.a.s.l), from July 2008 to July 2010. The data set represents the first year-round concurrent record of these compounds sampled at a high latitude Arctic site. Here, the study focused on the seasonal variability of these important ozone (O_3) precursors in the Arctic troposphere and the impact from transported anthropogenic and biomass burning emissions. Our analysis shows that PAN is the dominant NO_y species in all seasons at Summit, varying from 42 % to 76 %, however, we find that odd NO_y species (odd $NO_y = NO_y - PAN - NO_x$) contribute a large amount to the total NO_y speciation. We hypothesize that the source of this odd NO_y is most likely alkyl nitrates and nitric acid (HNO_3) from transported pollution, and photochemically produced species such as nitrous acid (HONO).

FLEXPART retroplume analyses and black carbon (BC) tracers for anthropogenic and biomass burning (BB) emissions were used to identify periods when the site was impacted by polluted air masses. Europe contributed the largest source of anthropogenic emissions during the winter months (November–March) with 56 % of the total anthropogenic BC tracer originating from Europe in 2008/2009 and 69 % in 2009/2010. The polluted plumes resulted in mean enhancements above background levels up to 334 $\mathrm{pmol\,mol^{-1}}$, 295 $\mathrm{pmol\,mol^{-1}}$, 88 $\mathrm{pmol\,mol^{-1}}$, and 1119 $\mathrm{pmol\,mol^{-1}}$ for NO_y, PAN, NO_x, and ethane, respectively, over the two winters. Enhancements in O_3 precursors during the second winter were typically higher, which may be attributed to the increase in European polluted air masses transported to Summit in 2009/2010 compared to 2008/2009. O_3 levels were highly variable within the sampled anthropogenic plumes with mean ΔO_3 levels ranging from -6.7 to 7.6 $\mathrm{nmol\,mol^{-1}}$ during the winter periods.

North America was the primary source of biomass burning emissions during the summer, however, only 13 BB events were observed as the number of air masses transported to Summit, with significant BB emissions, was low in general during the measurement period.

The BB plumes were typically very aged, with median transport times to the site from the source region of 14 days. The analyses of O_3 and precursor levels during the BB events indicate that some of the plumes sampled impacted the atmospheric chemistry at Summit, with enhancements observed in all measured species.

1 Introduction

The seasonality of ozone (O_3) and its precursors for photochemical production, such as nitrogen oxides, i.e. NO_x ($NO_x = NO + NO_2$), peroxyacetyl nitrate (PAN), and non-methane hydrocarbons (NMHC), in the remote Arctic troposphere is governed by a combination of transport pathways, photochemistry, and stratospheric influx (Klonecki et al., 2003; Stohl et al., 2006; Law and Stohl, 2007; Liang et al., 2011). Improving our knowledge on the seasonality of O_3 and its precursors and the relative importance of source regions and transport variability is essential as recent studies have suggested that tropospheric O_3 may have a large impact on radiative forcing and climate feedbacks in the Arctic region (Shindell et al., 2006; Shindell, 2007; Quinn et al., 2008).

Polluted air masses originating from anthropogenic and biomass burning sources in the mid-latitude regions can transport long-lived reservoir species of NO_x, such as PAN, and nitric acid (HNO_3), to the Arctic region (Wofsy et al., 1992; Wespes et al., 2012), which may reform NO_x and result in enhanced levels far downwind from the emission sources (Beine et al., 1997; Walker et al., 2010). NMHC may also be transported in air masses from anthropogenic and biomass burning sources. The mole fractions of NMHC in the Arctic atmosphere can vary greatly during the year due to seasonal variability in emissions, transport pathway variability and the reaction with OH radicals (Jobson et al., 1994; Blake et al., 2003; Swanson et al., 2003).

Studies of pollution plumes with airborne, satellite- and ground-based observations, and model simulations show that long-range transport from Europe and North America to the lower Arctic troposphere may constitute a large source of tropospheric O_3 and O_3 precursors, whereas at higher altitude, pollution plumes transported from Asia are an important

source (e.g. Atlas et al., 2003; Klonecki et al., 2003; Lamarque and Hess, 2003; Law and Stohl, 2007; Shindell et al., 2008; Fisher et al., 2010; Singh et al., 2010; Walker et al., 2012; Wespes et al., 2012; Bian et al., 2013). A large contribution to the seasonality of O_3 and O_3 precursors in the Arctic troposphere is due to variability in the location of the Arctic polar front (Klonecki et al., 2003; Stohl, 2006). During winter in the Northern Hemisphere, the polar front expands southward over North America, Europe and Siberia allowing direct transport of polluted air masses from sources within these latitudes to the Arctic. The Arctic polar front recedes in summer, reducing the impact of these pollution sources on the Arctic lower troposphere. However, it has been shown that the transport of emissions from biomass burning regions to the Arctic is possible during summer (Stohl, 2006) and that they can strongly impact the atmosphere above Summit Station in Greenland (Stohl et al., 2006). Results from a modeling study by Walker et al. (2012) using tagged emissions in the global chemical transport model GEOS-Chem show that during summer the primary emissions that impact the production of O_3 in the Arctic region were from high latitude regions, whereas, during the fall and winter periods, transport of emissions from mid-latitude regions in North America and Europe is possible.

A number of studies have discussed the seasonality of surface O_3 (Bottenheim et al., 1994; Beine et al., 1997; Monks, 2000; Browell et al., 2003; Helmig et al., 2007b; Walker et al., 2012), nitrogen oxides (Barrie and Bottenheim, 1991; Honrath and Jaffe, 1992; Bottenheim et al., 1994; Muthuramu et al., 1994; Beine et al., 1997; Solberg et al., 1997; Dibb et al., 1998; Munger et al., 1999; Beine and Krognes, 2000; Stroud et al., 2003; Thomas et al., 2011), and NMHC (Jobson et al., 1994; Blake et al., 2003; Klonecki et al., 2003; Swanson et al., 2003; Helmig et al., 2014) in the Arctic. However, due to the logistical difficulties in measuring at remote Arctic locations, the majority of seasonal studies have taken place at coastal sites in Northern Europe, Canada, and Alaska, or focused on the late spring/summer periods. Seasonal and interannual studies of nitrogen oxides in the remote Arctic troposphere are largely missing. The high latitude Arctic has negligible impact from local pollution sources, and local production of NO_x from PAN decomposition is expected to be small in this cold region. Therefore, enhanced mole fractions of nitrogen oxides are pri-

marily a result of long-range transported pollution from anthropogenic or biomass burning sources in Europe, North America, and Asia, or of downward transport from the stratosphere (e.g. Liang et al., 2011). Measurements within the boundary layer over Greenland ice sheet are also influenced by emissions from photochemical reactions within the snowpack (Grannas et al., 2007, and references therein), and variability in the boundary layer height (Cohen et al., 2007; Anderson and Neff, 2008; Van Dam et al., 2013), both of which may impact the observed NO_y budget and seasonal cycle of O_3 precursors in this region.

A build-up of O_3 precursors during winter in the Arctic free troposphere may have important implications for the tropospheric O_3 budget in the mid-latitudes during late spring and early summer (Gilman et al., 2010). Modeling studies have postulated that air masses originating from the Arctic region can result in the transport of NO_y and NMHC to the North Atlantic and enhance tropospheric O_3 in this region due to the thermal decomposition of PAN (Honrath et al., 1996; Hamlin and Honrath, 2002).

This study utilizes 2 years of continuous measurements and model results to characterize the seasonally varying magnitude of O_3 and its precursors in the remote high latitude Arctic and potential impact from transported pollution. Year-round measurements of NO_x, NO_y, PAN, O_3, and NMHC from the high altitude Greenland Environmental Observatory at Summit (GEOSummit) station in Greenland are presented. The paper is structured as follows: in Sect. 2, the techniques to measure NO, NO_2, NO_y (total reactive nitrogen oxides NO_y=NO+NO_2+PAN+HNO_3+HONO+others), PAN, and NMHC are presented and the FLEXPART Lagrangian particle dispersion model utilized in this study is discussed. Sect. 3.1 presents the seasonal cycles of O_3 precursors at the measurements site and the NO_y speciation is investigated. In Sect. 3.2, the source contributions to enhanced O_3 precursors from anthropogenic emissions and biomass burning are discussed. Finally, a summary of the main findings is given in Sect. 4.

2 Experimental methods

2.1 GEOSummit Station

Measurements of NO_x, NO_y, PAN, and NMHC were performed at the GEOSummit Station (hereafter called Summit), Greenland (72.34° N, 38.29° W, 3212 m.a.s.l), from July 2008 to July 2010. Inlets for the instruments were installed ∼8.5 m above the snowpack (∼6.5 m toward the end of the measurement period, as a result of snow accumulation) on a meteorological tower located approximately 660 m south-west of the main camp within the "clean air" sector. Tubing and cables were routed through a heated pipe to a buried laboratory facility.

2.2 Measurements

2.2.1 Nitrogen oxides

Measurements of NO, NO_2, and NO_y were performed with an automated O_3 chemiluminescence detection system (Ridley and Grahek, 1990). The instrument was developed at Michigan Technological University and is based on the same design that was used in Newfoundland in 1996 (Peterson and Honrath, 1999), subsequently installed at Summit during campaigns in 1998, 1999 and 2000 (Honrath et al., 1999, 2002; Dibb et al., 2002), and at the Pico Mountain Observatory from 2002 to 2010 (Val Martín et al., 2006). NO_2 and NO_y were detected by chemiluminescence after reduction to NO using a photolytic NO_2 converter (Kley and Mcfarland, 1980) and a gold-catalyzed NO_y converter in the presence of CO (Bollinger et al., 1983; Fahey et al., 1985), respectively. NO_y is given as the sum of reactive nitrogen oxides. In the Arctic, NO_y is primarily comprised of NO, NO_2, PAN, HNO_3, HONO and particulate nitrate (p-NO_3^-). For the instrument used in this study, a photolytic blue LED NO_2 converter (Air-Quality Design Inc., Colorado) was installed. Photolytic converters have lower conversion efficiencies than molybdenum converters, however, interferences from other species photolyzing to NO, such as HONO and PAN, are reduced

(Pollack et al., 2011; Villena et al., 2012). The sample mass flow controllers (MFC) and the NO_2 and NO_y converters were housed inside the inlet box on the tower to minimize the residence time of NO_y species inside the PFA tubing.

During each measurement cycle of 10 min, the NO and NO_2 signals were recorded as 30 s averages and NO_y signals as 20 s averages, after a period of equilibration in each mode. Zero measurements of NO were performed at the start and end of each measurement cycle by mixing O_3 with the sample upstream of the reaction chamber. The zero signals were measured to determine the interference signal in the reaction chamber, which was then subtracted from the measured signals. Calibrations were performed every 12 hours to determine the sensitivity of the instrument to NO via standard addition ($10\,cm^3\,min^{-1}$) of NO in nitrogen (N_2) (ranging from 0.792 - 0.930 $mmol\,mol^{-1}$, Scott Marrin, Scott Specialty Gases) to the sample flow of $650\,cm^3\,min^{-1}$ at the inlet on the tower. A known amount of NO_2, generated via gas phase titration of NO with O_3, was also added to the sample flow during the calibration cycle, to determine the conversion efficiencies of the NO_2 and NO_y converters. In addition to the standard calibrations, every three days the conversion efficiency of the NO_y converter to HNO_3 and n-propyl nitrate (NPN) were determined and artifacts for NO_y, NO, and NO_2 were measured via sampling NO_x free air (Breathing air grade, Airgas, Radnor, PA, USA). The final datasets were corrected for this artifact.

Approximately 7 % of the final NO and NO_2 datasets and 8 % of the final NO_y dataset were removed due to known instrument issues. Additional filtering procedures were applied to remove points potentially contaminated by local camp pollution. Variability in the 20 and 30 s averaged data was compared to the expected value from photon counting statistics which are treated as a Poisson distribution. Measurements with variability greater than 3 times the Poisson value were then removed from the final dataset (~ 5 %). Evaluation of these periods show that they typically occur when the wind direction was from the main camp, confirming that local pollution was the main source of the variability. Erroneous data points as a result of unknown instrument issues, or periods when the skiway was groomed, were also removed. Less than 0.2 % of the total data were classified as erroneous and each point was manually checked by comparing to adjacent observations. Finally, large negative

mole fractions, as a result of large variability between modes during the measurement cycle, were removed ($\lesssim$1 %).

The final NO, NO_2, NO_x, and NO_y data used in this work were further averaged over a 30 min period. NO_x was determined as the sum of the NO and NO_2 measurements during each 10 min cycle. The overall uncertainty for the 30 min data is calculated from the root sum of the squares of the measurement accuracy, artifact uncertainty, and precision. Maximum uncertainties for NO, NO_2, and NO_x at 50 pmol mol^{-1} are 10 %, 17 %, and 19 %. For NO_y, the total uncertainty is also dependent on the conversion efficiencies of the NO_y species, which is estimated to be $\sim$ 10 % based on the conversion efficiencies and NO_y levels expected at Summit. The total uncertainty in NO_y is estimated to be $\sim$ 12 % at 200 pmol mol^{-1}. Detection limits for the 30 min averages were estimated from the 2σ precision of the measurements, based on the standard error of the photon counting noise. Median detection limits for NO, NO_2, NO_x, and NO_y were 2.7 pmol mol^{-1}, 5.0 pmol mol^{-1}, 5.7 pmol mol^{-1}, and 3.8 pmol mol^{-1}, respectively. Mole fractions below the detection limit, including small negative mole fractions (as a result of uncertainties in the zero measurement and artifact corrections) were included in all averaging calculations to ensure the final values were not biased. Further details on the calibrations performed and the precision and accuracy of the measurements are provided in the supplement.

2.2.2 Peroxy-acetyl nitrate

A commercial PAN gas chromatography analyzer (PAN-GC, Metcon, Inc., Boulder, CO) was installed alongside the NO_{xy} instrument to determine atmospheric PAN mole fractions. The PAN instrument is based on gas chromatography with electron capture detection (GC-ECD). The instrument was equipped with a preconcentration unit to improve the detection limit whilst allowing for PAN sampling every 10 min. The preconcentration unit traps PAN and carbon tetrachloride (CCl_4) on a Peltier-cooled (5 °C) capillary column with subsequent desorption at approximately 35 °C for injection onto the main GC column, which was set to a temperature of 15 °C. Ultra-pure nitrogen gas (99.9999 % purity) was used as the carrier gas for the PAN-GC.

The instrument was calibrated approximately every week using a known concentration of PAN, which was photochemically produced from the same NO-calibration gas used for the NO_{xy} instrument described in Sect. 2.2.1. The PAN concentration was determined from the NO calibration gas mixing ratio, the mass flow rates and the conversion efficiency of NO to PAN, and varied from $\sim$520–700 pmol mol^{-1}, during the measurement period. The NO gas was delivered to a reaction cell inside the PAN calibration unit which contained a UV mercury lamp to photolyze an excess of acetone (in zero air) to form peroxyacetyl radicals that oxidize the NO gas to NO_2. NO_2 then reacts with peroxyacetyl radicals to form PAN. The PAN calibration gas was sent to the inlet on the tower and then sampled by the GC-ECD. The NO_{xy} instrument was used to determine the conversion efficiency of NO to PAN at the beginning and end of the measurement period. Some of the gas sent to the PAN inlet was redirected to the NO_{xy} instrument and the NO and NO_2 levels were measured with the PAN calibration unit switched on and off. The conversion efficiency remained relatively constant throughout the measurement period at $93 \pm 3\,\%$ (mean $\pm$ uncertainty).

Uncertainty in the PAN calibration is associated with uncertainties in (a) the calculation of the NO addition, (b) the conversion of NO to PAN in the calibration unit and, (c) variability in the PAN peak areas during the calibration. The root mean squared propagation of error gives an uncertainty in the calibration standard of 16 % during normal operation. The sensitivities determined from the weekly PAN calibrations were interpolated to the measurements to take into account any drifting. Additional uncertainty arises from short-term variability in sensitivity between calibrations. CCl_4 was used as an internal reference during periods when calibrations were not taken (Karbiwnyk et al., 2003). The atmospheric concentration of CCl_4 is relatively constant; therefore any changes in the CCl_4 peak area are primarily caused by changes in the instrument sensitivity. The median relative standard deviation (RSD) of the CCl_4 peak area between calibrations was 6 %. During a period between 14 February 2009 and 25 May 2009 there was a gap in the calibrations caused by a blockage in the tubing that delivered the PAN calibration gas to the inlet. To estimate PAN sensitivities during this period, the calibrations before and after the blockage were used to perform a linear regression between the PAN sensitivities and the CCl_4 peak areas. The

slope and intercept from the regression were then used to determine the PAN sensitivities from the CCl_4 peak areas between 14 February 2009 and 25 May 2009. An additional uncertainty in the PAN measurements of 12 % (median RSD) was estimated from errors in the regression. The total uncertainty in the PAN calibration is determined from the root sum of the squares of the uncertainties in the calibrations and the variability, giving an uncertainty of 17 % during normal operation, and 21 % during spring 2009.

The limit of detection (LOD) of the instrument was estimated from the peak to baseline noise ratio. The LOD is defined as the mole fraction giving a signal to noise (S/N) ratio of 3. The noise level was determined as the peak-to-peak value of the baseline noise from a region just after the PAN peak, for each chromatogram. The limit of detection was highest during the first few months of operation with a LOD up to 75 $\mathrm{pmol\,mol^{-1}}$ in September 2008. The LOD improved after November 2008, decreasing to around 20-40 $\mathrm{pmol\,mol^{-1}}$ from April 2009 until late January 2010. In spring 2010, the LOD increased to $\sim 40-65\,\mathrm{pmol\,mol^{-1}}$ as a result of drifting and a noisy baseline as the detector became dirty. Due to the degradation of the detector, no data after 28 April 2010 were included in the analyses here.

Similarly to the NO_x and NO_y data, the PAN measurements were averaged over 30 min. The total uncertainty for the 30 min averaged PAN mole fractions was determined from the root sum of the squares of the measurement precision (estimated as $2\sigma N^{0.5}$, where N is the number of points averaged in 30 min (N$\leq$ 3)) and from the uncertainty in the calibration. The precision was typically $<$26 $\mathrm{pmol\,mol^{-1}}$ with a mean (median) value of 6.5 $\mathrm{pmol\,mol^{-1}}$ (5.3 $\mathrm{pmol\,mol^{-1}}$). Using the median precision, the total uncertainty in the PAN measurements at 100 $\mathrm{pmol\,mol^{-1}}$ was estimated to be approximately 18 % during normal operation, and 22 % during spring 2009. For the statistical analyses presented here, 30 min avgs below the LOD were treated as 1/2 of the limit of detection. Despite the high LOD, $\sim$74 % of the 30 min avg PAN data were above the LOD during 2008 and $>$ 99 % were above the LOD from 2009 onwards. The final PAN data set was not filtered for wind direction as analyses showed that there was no obvious influence from camp pollution on the PAN measurements.

2.2.3 Non-methane hydrocarbons

NMHC were continuously sampled from June 2008 to July 2010 using a fully automated and remotely controlled GC system that was specifically designed for this study. Details of the setup at Summit are given in Helmig et al. (2014). The GC is a further development of the instrument operated at the Pico Mountain Observatory and described in detail by (Tanner et al., 2006). The NMHC system provided ~ 8 ambient measurements of C_2–C_6 hydrocarbons each day, with each measurement representing a collection/sample integration time during the sample pre-focusing step of ~ 45 min. In addition, one blank sample was analyzed $\sim$ daily, and a standard every ~ 2 days.

The inlet for the GC instrument was installed on the same tower as the PAN, NO_y, and NO_x inlets. The instrument relied on a cryogen-free sample enrichment and injection system. All consumable gases were prepared at the site with a hydrogen generator, compressor, and air purification system. Aliquots of the sample stream were first passed through a Peltier-cooled trap to dry the air to a dew point of $-30\,^{\circ}$C, then through an ozone scrubber, and NMHC were then concentrated on a Peltier-cooled ($-25\,^{\circ}$C) multi-stage adsorbent trap. Analysis was accomplished by thermal desorption and injection onto an aluminum oxide (Al_2O_3) porous layer open tubular (PLOT) column for cryogen-free separation on a SRI Model 8610 GC with flame ionization detection (FID). Blanks and standard samples were injected regularly from the manifold. The gravimetric and whole air standards that were used were cross-referenced against our laboratory scale for volatile organic compounds, which has been cross-referenced against national and international scales, including through two previous audits by the World Calibration Centre for VOC (http://http://imk-ifu.fzk.de/wcc-voc/). At 100 pptv mole fraction, analytical accuracy and precision were typically better than 3–5 %, yielding a combined uncertainty estimate of ~ 5 %. The instrument achieved low single digit pmol mol^{-1} detection limits. During summer, when NMHC levels for C_4–C_5 NMHC at times dropped below the detection limits, for the statistical and whisker plot calculations those data were treated as 1/2 of the detection limit.

2.2.4 Ozone

Surface O_3 was measured by an O_3 analyzer located in the Temporary Atmospheric Weather Observatory (TAWO) building a few hundred meters from camp by the National Oceanic and Atmospheric Administration (NOAA) as part of the core atmospheric measurements that began in 2000 (Petropavlovskikh and Oltmans, 2012). Hourly averaged data for 2008, 2009, and 2010 were downloaded from the Earth System Research Laboratory Global Monitoring Division (ESRL-GMD) website (http://www.esrl.noaa.gov/gmd/dv/data/).

2.2.5 FLEXPART

The Lagrangian particle dispersion model FLEXPART (version 8.2) was utilized to identify potential periods when polluted air masses impacted the measurement site. FLEXPART simulates atmospheric transport using wind fields from global forecast models to determine source to receptor pathways of air masses (Stohl et al., 2005). The model was driven with meteorological analysis data from the European Centre for Medium Range Weather Forecasts (ECMWF) and ran backward in time in so-called "retroplume" mode (Stohl et al., 2003). Every 3 h, 40 000 particles were released from the measurement site location and followed backwards in time for 20 days. Sensitivities to anthropogenic and fire emissions were determined during the backwards simulations and are proportional to the particle residence time over the source areas. In this work, a black carbon tracer was used to simulate both anthropogenic (BC_{anthro}) and biomass burning emissions (BC_{fire}). For the BC anthropogenic tracer the Emissions Database for Global Atmospheric Research (EDGAR) UNEP BC report 2005 data (UNEP, 2011; Shindell et al., 2012) was used. To estimate the BC fire emissions, MODIS hot spot data (Justice et al., 2002; Giglio et al., 2003) was used to estimate the area burned (180 hPa per MODIS hot spot) and combined with a combustion efficiency, emission factor, and fuel load, which were all based on land use type (Stohl et al., 2006). The land surface types are taken from the NOAH Land Surface Model version 2.7.1. Other factors are provided in Table S1 in the supplementary material. The BC tracer was susceptible to both wet and dry deposition during transport. The wet scavenging coefficient

used in the model is more representative of a hydrophilic aerosol, however, there is no conversion from hydrophobic to hydrophilic properties with aging BC in the model, therefore, greater scavenging may occur closer to the source region, resulting in an underestimation of the BC tracer at Summit (Stohl et al., 2013). However, for this study the tracer was only used to identify events; therefore, absolute BC values were not required. Carbon monoxide can also be used as a tracer for pollution transport. Simulations using CO were performed for the anthropogenic tracer, however, the BC tracer was used in this study as simulations were available for both anthropogenic and fire tracers as part of the POLARCAT campaign, and thus allowed for consistency between the biomass burning and anthropogenic analysis. A comparison was made between the CO and BC anthropogenic tracers to determine whether pollution events were missed when using the BC tracer, as a result of deposition. A time series and correlation plot for the two tracers from summer 2008 to 2010 are shown in Figures S1 and S2 in the supplementary material. The result suggests that although there may be some differences in the magnitude of the FLEXPART tracers, the transport simulated with the BC tracer correlates well with the CO tracer (Pearson's correlation coefficient, R=0.97), therefore, significant pollution events were unlikely to be missed.

3 Results and discussion

3.1 Seasonal cycles

3.1.1 Reactive nitrogen oxides

Figure 1a–d shows the statistical analyses of the monthly averaged NO_y, NO_x, PAN, and O_3 ambient mole fractions, respectively, during the measurement period from July 2008 to July 2010. A malfunction with the NO_{xy} instrument resulted in missing NO_x and NO_y data from 24 November 2008 to 30 March 2009. Seasonal cycles are observed for all measured species, with higher levels during the late winter/early spring period and lower mole fractions from summer to fall. The positively skewed whiskers indicate that air masses with elevated

levels of NO_x, NO_y, and PAN, were sampled year-round. Anthropogenic and biomass burning emissions transported to the site from North America and Europe are a major source of these enhancements (see Sect. 3.2). Observations from the Arctic Research of the Composition of the Troposphere from Aircraft and Satellites (ARCTAS) mission in 2008 show that mixed stratospheric-tropospheric air masses, above 5 km, have elevated levels of O_3 precursors such as NO_x and HNO_3, which can subsequently be converted to PAN (Liang et al., 2011). Therefore, high mole fractions observed in PAN, NO_y, and NO_x, may also be the result of sampling air masses mixed with those originating from the stratosphere and upper troposphere.

Table 1 gives a statistical summary for the monthly averages of PAN, NO_y, NO_x, and O_3 during 2008–2010. Maxima in monthly mean mole fractions of PAN occur in April with mean levels of 217 ± 65 (1σ) pmol mol^{-1} and 273 ± 100 pmol mol^{-1}, for 2009 and 2010, respectively. The difference between monthly mean PAN levels observed in April 2010 and April 2009 are within the measurement uncertainties (as shown in Figure S3, supplementary material), however, the 30 minute averages (shown in Figure S4) indicate high levels of PAN, NO_y, and NO_x in April 2010. These high levels are explored further in Sect. 3.2.1. Monthly mean NO_y mole fractions also peaked during April 2010 at 352 ± 102 pmol mol^{-1}. PAN mole fractions at Summit and the magnitude of the PAN springtime peak are consistent with observations at other high latitude sites such as Zeppelin Mountain, Svalbard (Beine et al., 1997; Solberg et al., 1997; Beine and Krognes, 2000), and Alert, Northwest Territories, Canada (Worthy et al., 1994; Dassau et al., 2004). PAN levels in September 2008 were very low and typically below the detection limit as a result of a noisy baseline. In 2009, PAN reached a monthly minimum of 63 pmol mol^{-1} in July. NO_y mole fractions did not decrease as quickly as PAN from spring to summer in 2009 and reached a minimum monthly average during September. We find that the PAN and NO_y summer mole fractions observed here are comparable to previous measurements performed at the same site in 1998 and 1999, when observed PAN levels were typically 20–150 pmol mol^{-1}, and NO_y levels ranged between 100–300 pmol mol^{-1} (Honrath et al., 1999; Ford et al., 2002). The slower decrease in NO_y from spring to summer, compared to PAN, is a result of the presence of NO_x and

odd NO_y (odd $NO_y = NO_y - PAN - NO_x$) over the summer months and is discussed further below.

The seasonal cycle of PAN is governed by the rate of thermal decomposition and transport patterns. The warmer summer temperatures result in the decomposition of PAN during long range transport; additionally, during the summer months the polar front recedes north, thus reducing the potential for anthropogenic emissions to reach the measurement site (Beine and Krognes, 2000; Stohl, 2006). Measurements have shown that PAN is typically the largest contributor to NO_y in the Arctic, due to the rapid formation of PAN near the source region and a long lifetime in the free troposphere (Solberg et al., 1997; Munger et al., 1999; Ford et al., 2002; Alvarado et al., 2010; Singh et al., 2010; Liang et al., 2011). However, there have been very few studies on the seasonal variability of the NO_y speciation in the Arctic due to limited measurements over winter months.

The full annual cycle of NO_y contributions from PAN and NO_x during this study provides some information on the NO_y speciation, year–round, at Summit. Table 1 shows that PAN is the dominant form of NO_y all year, with monthly mean $[PAN]/[NO_y]$ ratios above 50 % in spring and fall, reaching a maximum of 76 % in April 2009. The lowest $[PAN]/[NO_y]$ ratios occurred during the summer, with a minimum monthly mean of 42 % in July 2008. The seasonal cycle for NO_x does not follow PAN and NO_y at Summit. As shown in Table 1, monthly mean NO_x levels peak one month later than NO_y and PAN, coinciding with an increase in solar radiation. Thus, the contribution of NO_x to NO_y maximizes over the summer (10–15 %). The monthly average NO_x contribution decreased to $\lesssim 3$ % over winter and typically NO_x levels were below the detection limit of the instrument. The thermal decomposition of PAN is a possible local source of ambient NO_x during spring and summer months (Beine et al., 1997), however, the ambient temperatures during the measurement period were always below freezing. The PAN lifetime at Summit is nearly two days at 0 °C (Sander et al., 2011), therefore, the contribution to NO_x from thermal decomposition at the site is expected to be very low.

Studies have hypothesized that photochemical reactions within the snowpack result in the release of NO_x and also HONO to the overlying atmosphere (e.g., Honrath et al., 1999,

2000a, b, 2002; Munger et al., 1999; Beine et al., 2002; Dibb et al., 2002; Dominé and Shepson, 2002; Beine et al., 2003; Grannas et al., 2007; Thomas et al., 2011). Thus, the increase of ambient NO_x with radiation in spring suggests a possible photochemical source. The diurnal cycles of ambient NO_x at Summit (discussed further below) also indicate a photochemical source of NO_x from the snowpack.

Fig. 2 shows the monthly averaged mole fractions of NO_y and PAN+NO_x during the measurement period. The results show that the sum of PAN and NO_x cannot always account for the monthly averaged NO_y within the measurement uncertainty range, suggesting a significant source of odd NO_y at Summit. When considering the 30 minute averages above the limit of detection for NO_x, NO_y and PAN, $\sim$ 46% of the data show significant odd NO_y levels (i.e. cannot be accounted for by total measurement uncertainty alone). What is particularly striking about the NO_y speciation is that odd NO_y levels can be very large over winter (Fig. 3). The monthly mean odd NO_y reached 110 ± 37 pmol mol^{-1} (mean $\pm$ uncertainty) in February 2010. The peak in odd NO_y was in March 2009 at 126 ± 48 pmol mol^{-1}, however, the data may be bias as there were only 34 coincident NO_x, NO_y, and PAN measurements in March 2009, whereas there were between $\sim 270-1200$ coincident measurements during the other months. Odd NO_y decreased to $\sim 20-60$ pmol mol^{-1} over the summer months; however, this still accounts for up to ~ 40 % of the total NO_y during this period. Snowfall rates increase during the summer months at Summit (Dibb and Fahnestock, 2004), therefore, an increase in deposition of water-soluble species such as HNO_3 to the snowpack may result in the depletion of ambient odd NO_y in the summer. The increase in solar radiation may also play an important role in the reduction of odd NO_y species in the summer. Solberg et al. (1997) observed a decrease in odd NO_y with increasing solar UV radiation in Spitsbergen, Norway. The authors suggested that species such as HONO, HNO_3, NO_3, N_2O_5, HO_2NO_2, and alkyl nitrates may contribute to NO_y over the winter with the impact reducing in spring due to an increase in photolysis. A study on the seasonal variability of alkyl nitrates at Summit in 1998–1999 found that the light C_1–C_4 alkyl nitrates peaked over winter (Swanson et al., 2003). The monthly mean total C_1–C_4 mole fraction during February 1999 was 33 pmol mol^{-1}. Assuming a similar level during February 2010, alkyl nitrates

would account for $\sim 1/3$ of the odd NO_y observed during this month. Taking into account measurement uncertainties, there remains, therefore, a large fraction of NO_y unaccounted for over winter.

Results from this study show, despite the odd NO_y levels decreasing from late spring to summer, odd NO_y species can contribute over twice as much as NO_x to the total NO_y in summer. To investigate the source of the odd NO_y species and the possible impact from snowpack photochemistry we analyzed the ambient diurnal variability of NO_x, NO_y, and odd NO_y at Summit separately for March, April, May, and June, 2008–2010 (Fig. 4).

A clear diurnal cycle is observed in the NO_x, NO_y, and odd NO_y measurements in April and May. The NO_x diurnal cycle shows a minimum in the morning and peaks after solar noon. Diurnal cycles for NO and NO_2 are given separately in the supplementary material and show NO similarly peaking around solar noon. In contrast, NO_2 levels reach a maximum overnight. The observed NO_x cycle is in agreement with the cycle observed at Summit during summer 2000 (Honrath et al., 2002), which was attributed to photochemical reactions in the snowpack and enhanced vertical mixing during the day. Studies have shown that diurnally varying radiation at Summit can result in heating at the surface and the development of unstable to near-neutral conditions (Cullen and Steffen, 2001) and increasing boundary layer depths during the day (Helmig et al., 2002; Cohen et al., 2007), with entrained air having the effect of diluting snowpack emissions near the surface. Consequently, increased mixing may offset increased daytime surface fluxes or production rates and dampen or offset diurnal concentration cycles in the surface layer.

The amplitude of the diurnal cycles (determined as the difference between the minimum and maximum 2 h median values), was always greater for NO_y than NO_x from March to June. The NO_y and NO_x amplitudes were largest in May, with values of 35 $\mathrm{pmol\,mol^{-1}}$ and 22 $\mathrm{pmol\,mol^{-1}}$, respectively. The diurnal cycle for odd NO_y in May was 20 $\mathrm{pmol\,mol^{-1}}$, peaking around solar noon (Fig. 4k), suggesting a photochemically produced odd NO_y species may be present. It has been hypothesized that HNO_3 and HONO, may account for some of the NO_y diurnal variability at Summit (Ford et al., 2002). At Neumayer, Antarctica, the diurnal variability in NO_y was attributed to both boundary layer changes and snowpack-air

exchange of gases (Weller et al., 1999; Grannas et al., 2007). There is a possible contribution to the odd NO_y diurnal cycle in the summer at Summit from long range transport of pollution. Reactive nitrogen species such as HNO_3 and alkyl nitrates as these species have previously been observed in anthropogenic and biomass burning plumes in the Arctic (Liang et al., 2011; Wespes et al., 2012) and the downward transportation of pollution from aloft due to a growing boundary layer may result in a daytime maxima in NO_x and NO_y, which then decreases at night due to surface uptake.

Ambient HNO_3 and HONO have been measured at Summit during a number of spring and summer campaigns. Levels of HNO_3 are typically on the order of a few tens $\mathrm{pmol\,mol^{-1}}$, and HONO levels are lower with mole fractions of $\sim 10\ \mathrm{pmol\,mol^{-1}}$ or less (Dibb et al., 1994, 1998; Honrath et al., 1999; Dibb et al., 2002; Ford et al., 2002; Yang et al., 2002; Dibb et al. , 2007; Chen et al., 2007; Liao et al., 2011). Median mixing ratios of HNO_3 and HONO, measured during May and June, 2010, with a mist chamber/ion chromatography (MC/IC) system (~ 1.5 m above the snowpack), were 7 $\mathrm{pmol\,mol^{-1}}$ and 13 $\mathrm{pmol\,mol^{-1}}$, respectively (J.E. Dibb and M.G. Hastings, personal communication). Note that HONO measurements by MC/IC in polar regions should be viewed as an upper limit to the true value, due to potential interferences from other species (Chen et al., 2004; Liao et al., 2006). A direct comparison of HNO_3 and HONO with calculated odd NO_y levels is not possible for 2010 because PAN measurements were unavailable after April. Monthly mean odd NO_y levels calculated for May and June in 2009 were 43 and 36 pmol $\mathrm{mol^{-1}}$, respectively. Summer levels of alkyl nitrates are expected to be low at Summit with Swanson et al. (2003) measuring monthly mean levels (total C_1–C_4) of $\sim$ 10–20 $\mathrm{pmol\,mol^{-1}}$ between May and August. Assuming alkyl nitrate levels of $\sim$15 $\mathrm{pmol\,mol^{-1}}$ during May/June, the sum of HNO_3+HONO+alkyl nitrates are comparable to the odd NO_y levels measured at Summit, in May/June (when considering measurement uncertainties). Particulate nitrate may also contribute a small amount to the total NO_y, however, this contribution is expected to be small as ambient p-NO_3^- levels are typically lower than HNO_3 at Summit (Dibb et al., 1994).

HO_2NO_2, may also contribute to the odd NO_y measured at Summit. The partitioning of HO_2NO_2 between air and ice has a strong temperature dependence (Ulrich et al., 2012)

and a recent study in Antarctica, during polar winter, has shown that absorbed HO_2NO_2 can be emitted into the atmosphere above the snowpack when temperatures increase (Jones et al., 2014). HO_2NO_2 was also investigated as a possible source of NO_y during the Tropospheric Ozone Production about the Spring Equinox (TOPSE) campaign Stroud et al. (2003). Modeled HO_2NO_2 during February was comparable to the observed NO_y deficit of 60 pmol mol^{-1} between 3 and 6 km, however, the authors also note that the modeled HO_2NO_2 increased during May, while the observed NO_y deficit had decreased. It is apparent that further measurements are required to determine both the species and sources of this odd NO_y observed at Summit during winter.

In summary, the seasonal and diurnal cycles of NO_x and NO_y at Summit show that PAN is the dominant NO_y species in this region year-round, however, NO_x is an important contributor to the NO_y budget in summer. Local thermal decomposition of PAN is unlikely at Summit, due to the cold temperatures, therefore, the NO_x observed during summer is likely to be the result of upward emissions from the snowpack. Long-range transport may also play a role, as Summit is also influenced by pollution plumes that are mixed into the boundary layer (discussed further in Section 3.2). During spring and summer the NO_y observed at Summit can be attributed primarily to PAN, NO_x, HONO and HNO_3. Over winter, PAN is the dominant NO_y species, and alkyl nitrates are also likely to contribute to the observed NO_y, however, there is still a large fraction of NO_y that is unaccounted for over winter, and requires further investigation.

3.1.2 Non-methane hydrocarbons

Figure 5 shows the results for the C_2–C_5 alkane NMHC measured during 2008–2010 at Summit in ambient air. Measurements of primarily firn air conducted with this system were presented by Helmig et al. (2014). NMHC show a strong seasonal cycle with maximum mole fractions during the winter and early spring period and a rapid decline towards the summer, due to an increase in photochemical processing. The monthly averages for the C_2–C_5 NMHC are given in Table 2. During the summer period, measured mole fractions of the heavier NMHC were below or close to the detection limit. As expected, the phase of

each NMHC is shifted due to the rate of reaction with OH. The lightest of the NMHC shown in Fig. 5a, ethane (C_2H_6), peaks in March with a monthly mean of 2100 ± 151 pmol mol^{-1} (mean $\pm 1\sigma$) in 2009, and 1835 ± 174 pmol mol^{-1} in 2010, and declines to a minimum of $\sim$600 pmol mol^{-1} in July/August. Heavier NMHC have lower mole fractions, peak earlier in the year, and reach a minimum earlier in summer due to their faster rate of reaction with OH.

A comparison between the two winters shows monthly mean NMHC levels were consistently higher from November–March 2008/2009 when compared to 2009/2010. However, the standard deviation values during the second winter are typically higher, suggesting greater variability in the NMHC levels in 2009/2010. The non-averaged NMHC data (Figure S6, supplementary material), show there is considerable short term variability in the NMHC mole fractions superimposed on the seasonal cycle, in particular during the winter months. Short term elevated NMHC levels were observed during both winters and indicate fast transport of polluted air masses to the site.

The accumulation of O_3 precursors, such as nitrogen oxides and NMHC over winter has been suggested as a potential in situ source of O_3 that may contribute to the tropospheric O_3 peak (e.g., Penkett et al., 1993; Honrath et al., 1996; Monks, 2000; Blake et al., 2003). Results from studies during the TOPSE Atlas et al. (2003), have shown that the photochemical production of O_3 is important in the Arctic troposphere and can contribute more to the springtime O_3 budget than O_3 influx from stratosphere-troposphere exchange (Browell et al., 2003; Emmons et al., 2003).

The seasonality of NMHC can provide some insight into the potential for the photochemical production of O_3 in the Arctic troposphere during spring. Measurements of NMHC and O_3 during TOPSE show that within the mid-troposphere, total NMHC decreased by ~ 6.2 ppbC from February to May, and that O_3 increased by ~ 16 ppbv during the same period (Blake et al., 2003). The data from this study show similar results for NMHC, with the sum of the C_2–C_6 NMHC decreasing by ~ 4.5 ppbC from February to May. The magnitude of the O_3 increase, at ~ 8 ppbv, is smaller than observed during TOPSE, however, the

photochemical processing of NMHC in spring may contribute to the spring time peak of O_3 over Greenland.

3.2 Variability in ozone and its precursors from anthropogenic and biomass burning emissions

In Sect. 3.1, the seasonal cycles for O_3 precursors at Summit were discussed. Short term enhancements in O_3 precursor levels indicated that the boundary layer over Summit was often impacted by polluted air masses from lower latitudes. In this section the interannual and short term variability in the measured species at Summit, from 2008–2010, as a result of changes in transport pathways and the relative source contributions of pollutants from North America, Europe, and Asia are investigated.

Fig. 6 shows the total monthly averaged FLEXPART tracer simulations for BC_{anthro} and BC_{fire} tracers for 2008, 2009, and 2010. The data show that anthropogenic pollution impacts started to increase in November, peaking over the dark winter period, and then decreased in late spring. The total BC_{anthro} tracer at Summit is dominated by emissions from North America, Europe, and Asia. Source contributions from each continent can vary month-to-month and year-to-year, however, European emissions were typically the largest contributor to the total monthly BC_{anthro} during the winter period, when the polar front recedes northwards. During winter (NDJFM) 2008-2009, 56 % of the total BC_{anthro} originated from Europe, with 33 % from North America and 11 % from Asia. The following winter (NDJFM 2009-2010), European emission were higher at 69 %, with North America and Asia contributing 19 % and 11 %, respectively. A very small contribution ($\lesssim 1\%$) of the total anthropogenic tracer originated from other continents. Fig. 6 shows that the contribution to the total BC_{anthro} from Asia is low year-round. Hirdman et al. (2010) investigated the contribution of pollutants from different sources to various Arctic surface sites from 2002-2007. The authors show that Summit is less sensitive to emissions from the surface in the Arctic region, than low elevation surface stations, and air masses transported to Summit from outside of Greenland are likely to originate from Europe and North America.

In contrast to the anthropogenic tracer, North American emissions dominated the total BC_{fire} tracer, with 69 % of the total BC_{fire} tracer originating from this region from July 2008 to July 2010. This result is expected as air masses arriving at Summit typically originate from North America during the summer months (Kahl et al., 1997). Previous studies have also shown that North America is a major source of biomass burning emissions transported to Summit (e.g., Whitlow et al., 1994; Legrand and de Angelis, 1996; Fuhrer and Legrand, 1997; Alexander et al., 2004; Stohl et al., 2006).

The high Asian contribution to the total BC_{fire} tracer in spring 2008 is in agreement with observations during the POLARCAT campaigns in 2008, when a number of biomass burning plumes were observed from Siberia (Law et al., 2014, and references therein). During the measurement period, however, the contribution from Asian biomass burning emissions at Summit was low, compared to North America. European biomass burning emissions were also low, except during a period in March, when European fires dominated the total BC_{fire} tracer. In 2008 and 2010 the contribution from total biomass burning emissions peaked in August. In 2009, however, there was no significant peak in biomass burning emissions at Summit, and BC_{fire} tracer levels during the summer were much lower overall.

Variability in BC_{fire} tracer can be a result of a change in emissions or transport pathways. Overpass and cloud-corrected MODIS Terra (MOD14CMH) and Aqua (MYD14CMH) fire pixel counts from the Climate Modeling Grid (CMG) product were downloaded from the University of Maryland ftp server (ftp://fuoco.geog.umd.edu) to investigate the variability in fire emissions. The monthly total fire pixel count and total Fire Radiative Power (FRP), over the zonal region 40-75 N, were determined from March to September for 2008, 2009, and 2010 separately. The results (Figures S7a-d, supplementary material) show that there was a reduction in total fire counts and FRP in summer 2009, when compared to 2008 and 2010.

In the next two sections, the impact of anthropogenic and biomass burning emissions on O_3 and O_3 precursors are investigated.

3.2.1 Anthropogenic impacts

To investigate the source of the observed variability and the impact on ozone precursor levels, the anthropogenic tracer from FLEXPART retroplume simulations (BC_{anthro}) and NMHC emissions ratios were used to determine changes in the transport pathways and relative source contributions of anthropogenic emissions from different continents.

An event with pollution transport was defined as identified when the BC_{anthro} tracer was greater than the 75th percentile of the total BC_{anthro} during the 2 year measurement period (corresponding to $BC_{anthro} > 0.0082\,\mathrm{pmol\,mol^{-1}}$) for a minimum of 12 h. The FLEXPART temporal resolution for backward simulations is 3 h, so identifying events when the BC_{anthro} was enhanced for at least 12 h ensured that significant polluted air masses impacted the site. Using these thresholds, 85 anthropogenic pollution events were observed during the measurement period. Details for each event, including start date, FLEXPART tracer levels, and trace gas enhancements are presented in Table S2 in the supplementary material. The mean weighted age of the plume was also calculated for each FLEXPART retroplume, to determine the typical transport time for the events. As shown in Fig. 6, anthropogenic impacts are observed year-round, however, during the summer anthropogenic pollution events can be mixed with biomass burning emissions. Therefore, for this study, the focus is on events between November and March when FLEXPART anthropogenic tracer levels peaked and biomass burning emissions were typically low. In total, 52 events were identified during the periods November to March 2008/2009 (events 12-37) and November to March 2009/2010 (events 55-80). Typical mean transport times for polluted air masses in winter were $\sim 11-12$ days.

During each event, the mean ΔPAN, ΔNO_y, ΔNO_x, ΔO_3, and ΔC_2H_6 were calculated, where Δ is the enhancement above background levels (determined as the 20th percentile for each species, for each month and year). Care must be taken when defining a background level as the enhancement ratios are strongly dependent on this value. Initial analyses used a single background value for each month, determined from the 20th percentile of data from all years, however, this resulted in many negative or low enhancement ratios which were not

consistent with the observations. A background value for each individual month and year was found to be more appropriate, as these levels change slightly from year to year. For the 52 anthropogenic events identified during winter, the median (and range) value of the enhancements were 38 (-22 to 295) $\mathrm{pmol\,mol^{-1}}$ for PAN, 6.6 (-1.9 to 88) $\mathrm{pmol\,mol^{-1}}$ for NO_x, 67 (-17 to 334) $\mathrm{pmol\,mol^{-1}}$ for NO_y, 1.2 (-6.7 to 7.6) $\mathrm{nmol\,mol^{-1}}$ for O_3, and 142 (-245 to 1119) $\mathrm{pmol\,mol^{-1}}$ for C_2H_6.

Tests were performed to determine whether temporal mismatches occurred between the simulated plume arrivals and peaks in the measured species as a result of errors in the wind fields used in FLEXPART. Each event identified above was extended in time by 3, 6, 9, and 12 hours prior to and after the event, and new Δ values for the O_3 precursors were calculated. The analyses showed that extending the event window did not have a large impact on the mean Δ values when mole fractions were low, i.e. levels were typically near the background already and extending the event time did not result in additional plumes being captured. During those events with large peaks in O_3 and precursors, Δ values decreased, with increasing window lengths as a result of capturing lower background levels. Thus, the event times calculated using the original threshold appear to be in agreement with the pollution plume arrival times.

Over the two winters, negative mean ΔNO_y values were observed during 3 events (event 72, 78, and 79), negative ΔPAN during 4 events (18, 25, 72, and 73) and negative ΔC_2H_6 during 4 events (64, 72, 73, and 79). Negative Δ values were associated with, 1) events when the peak BC_{anthro} level was low (relative to BC_{anthro} peak levels during all events), indicating a small impact from anthropogenic pollution, 2) missing data points during the event, or 3) events when small enhancements in PAN and NO_y occurred, however, low mole fractions were also observed during the same event period.

Analyses of ΔO_3 and FLEXPART BC tracer masses show decreases in O_3 (ΔO_3 $<0\,\mathrm{nmol\,mol^{-1}}$), coinciding with anthropogenic pollution events, were observed during 20 periods in total from July 2008 to July 2010, with 16 of these events occurring between November and March, when sunlight is at a minimum. Negative ΔO_3 do not always coincide with low O_3 precursor levels. For example, Figure 7 shows a time series of mea-

surements between January 10 and March 2, 2010. During this period, events with elevated ethane, NO_y, PAN, and NO_x levels are clearly correlated with enhancements in the FLEXPART BC tracer, suggesting polluted air masses impacting the site; however, what is particularly striking is that O_3 mole fractions were low during some events (e.g. events 70, 71, and 74). Studies have shown that NMHC ratios can provide an indication of the photochemical aging of the air mass as the rate of reaction of different NMHC, and hence the ratio, is dependent on the amount of photochemical processing that occurs during transport (Parrish et al., 2004; Helmig et al., 2008; Honrath et al., 2008). High photochemical processing results in a decrease in the ln([propane]/[ethane]) ratio as propane reacts more readily with OH than ethane. The two low ozone events, during this period, with the largest ethane enhancements (70 and 71) on 22 and 29 January, coincided with enhancements in the ln([propane]/[ethane]) ratio, suggesting low photochemical processing, and fresher air masses, i.e. air that was subjected to more recent pollution before reaching at the site. It is difficult to obtain absolute air mass ages from NMHC ratios, due to dilution of the measured species during transport, however, the enhancements in the ln([propane]/[ethane]) ratio during the two pollution events coincide with sudden decreases in the mean weighted age of the plumes, estimated from FLEXPART. The vertically integrated emission sensitivity (also called the total column sensitivity, measured in nanosecond meters per kg) simulated by FLEXPART, was used to determine the air mass transport pathway.

Fig. 8a), shows the total column sensitivity from FLEXPART on 23 January (during event 70). The air mass originated from Northern Europe and resided in the lower $\sim 2\,\mathrm{km}$ during transport, until 1 day upwind when the air mass ascended over the surface of the Greenland ice sheet to the measurement site. Mean ΔPAN and ΔC_2H_6 levels during this event were 125 $\mathrm{pmol\,mol^{-1}}$ and 1036 $\mathrm{pmol\,mol^{-1}}$, respectively, supporting the FLEXPART analyses indicating a polluted air mass was sampled (note there was no NO_y data available during this period). Note that NO_x was also enhanced (mean ΔNO_x=87.7 $\mathrm{pmol\,mol^{-1}}$) during this event. As the air mass resided in the lower atmosphere before transport to the site, where temperatures are warmer, the enhanced NO_x observed is likely to be the result of PAN decomposition during transport. Ozone decreased, on average, 6.0 $\mathrm{nmol\,mol^{-1}}$

below the monthly background ($O_{3(bkg)} = 45\,nmol\,mol^{-1}$), and reached a minimum level of 35.4 $nmol\,mol^{-1}$. In contrast, a few hours later the transport patterns quickly changed, and the air masses sampled at Summit originated from high altitudes over North Canada, as shown in Fig. 8b. As a result, O_3 levels increased and NO_x, PAN, and ethane all decreased. Air originating from the high Arctic region was sampled at the site until 29 January, when the air transport moved southward, and air masses residing in the lower troposphere over North America transported polluted air to Summit (Fig. 8c). From 29–30 January (event 71), ethane, NO_y, PAN, and NO_x all increased with mean enhancements of 1119, 184, 92.1, and 10.6 $pmol\,mol^{-1}$, respectively. The mean ΔO_3 during event 71 was -0.7 $nmol\,mol^{-1}$, reaching a minimum O_3 level of 39.6 $pmol\,mol^{-1}$.

Background O_3 levels at Summit are typically higher than those observed at lower elevation Arctic sites due to a stronger influence of transport from the stratosphere, a reduction in ozone depletion events from halogens, and low surface deposition rates (Helmig et al., 2007a, b; Hirdman et al., 2010). The decrease in O_3 observed during winter/early spring is likely to be the result of titration of O_3 by NO within the sampled air mass soon after emission (Eneroth et al., 2007; Hirdman et al., 2010) and reduced mixing with the background air. FLEXPART retroplume analyses indicate that low O_3 events over winter typically coincide when sampling air masses originating from either Europe or North America, which have resided in the lower troposphere and/or are quickly transported over the Greenland ice sheet to the measurement site (examples of FLEXPART retroplumes are shown in Fig. S8a–e in the supplement). In contrast, periods identified during winter as pollution events with positive O_3 enhancement values often occurred when the air masses resided in the mid-troposphere during transport to the site (Fig. S9a-e), thus allowing for greater mixing with air from high tropospheric or stratospheric origin.

To investigate interannual variability in emissions and their impact on O_3 and O_3 precursors, a comparison of the enhancement values for ΔO_3, ΔPAN, and ΔC_2H_6 was made over the two winters (no comparison was made for NO_x or NO_y as measurements were limited during winter 2008/2009). Results show that enhancements in O_3 and O_3 precursors during events were typically higher during the second winter season, with median (mean) values of

12 (37) pmol mol^{-1}, 126 (162) pmol mol^{-1}, and 0.7 (1.2) nmol mol^{-1} in 2008/2009, and 51 (56) pmol mol^{-1}, 178 (237) pmol mol^{-1}, and 1.4 (1.3) nmol mol^{-1} in 2009/2010, for ΔPAN, ΔC_2H_6, and ΔO_3, respectively. FLEXPART analyses, presented in Sect. 3.2, show that European emissions contributed a greater amount to the anthropogenic air masses arriving at Summit in winter 2009/2010 compared to the previous year, thus, the higher enhancements are consistent with expectation that European emissions have a larger impact on the Arctic lower atmosphere in winter than North America or Asia.

In this study, the impact from anthropogenic emissions, as identified through FLEXPART retroplume analyses, were the primary focus. However, enhancements in the measured species were also observed during periods which are not correlated with pollution events simulated by FLEXPART. For example, on 15 February and 24-28 February 2010, (Fig. 7), enhancements in PAN, NO_y, and ethane are observed that do not coincide with high FLEXPART BC_{anthro} tracer levels. The BC_{fire} tracer from FLEXPART during this period is low, suggesting that the event was not the result of biomass burning emissions. The retroplume shows the air masses from these two events were transported over north Canada and remained in the Arctic for many days before arriving at Summit (not shown here). It is unlikely that the air sampled was from stratospheric origin, as ethane levels were high and ozone decreased during these events. It is possible that there may be missing sources in FLEXPART, or that the pollution originated prior to the 20 day simulation.

Enhancements in O_3 precursors that do not coincide with high FLEXPART tracer simulations were also observed during the spring months, however, O_3 was typically enhanced during these events, suggesting a different source than those in February 2010. FLEXPART analyses indicate the air masses were well aged, therefore, mixing with air masses originating from the upper troposphere/stratosphere is possible. For example, the highest PAN and NO_y levels during spring 2010 were observed between 22-24 April, when FLEXPART retroplumes show that the air masses were transported between 3300 and 4300 m.a.s.l (Fig. 9). During this same period, ethane and O_3 were also high. This event may be an example of tropospheric air, with high levels of NMHC, mixing with stratospheric air rich in O_3 and NO_y, resulting in PAN formation (Liang et al., 2011). The determination of the sources that result

in enhancements in O_3 and its precursors, that cannot be attributed to pollution transport, requires further investigation.

The study here has focused on anthropogenic impacts during the winter period as this is when FLEXPART anthropogenic tracers peak, however, it should be noted that high ΔO_3 events occurred in the summer months, in particular between between May and August. Some of the anthropogenic air masses were mixed with BB plumes (as discussed in the next section), however, the largest enhancement in O_3, during the measurement period (ΔO_3=15.0 $\mathrm{nmol\,mol^{-1}}$), occurred from June 4-8 2009, as a result of transport of anthropogenic emissions from Europe to Summit in $\sim$10 days. O_3 precursors were also enhanced during this event, indicating that further O_3 production may be possible during subsequent transport.

3.2.2 Biomass burning impacts

The extended whiskers shown on the plots in Fig. 1 indicate a large amount of variability in the O_3 precursors during the summer months. Radiation, surface emissions, boundary layer height, and changes in air mass sampling may all contribute to the variability observed. Anthropogenic emission impacts tend to be lower in the summer as a result of reduced transport from source regions, as shown in Fig. 6, however, pollution from anthropogenic and, especially, BB emissions can still impact the center of Greenland (Stohl, 2006), resulting in elevated mole fractions for short periods (Stohl et al., 2006). Studies based on aircraft measurements and models during the ARCTAS campaigns in both spring and summer 2008 show that NO_x, NO_y, PAN, and hydrocarbons levels can be elevated in biomass and anthropogenic plumes transported to the Arctic(e.g. Alvarado et al., 2010; Singh et al., 2010; Hornbrook et al., 2011; Liang et al., 2011).

The BC_{fire} tracer from FLEXPART was used to identify periods at Summit that were potentially impacted by BB emissions. Potential inaccuracies with the FLEXPART simulation of transport pathways, fire identification, and tracer emission uncertainties may result in BB events being under or overestimated, however, FLEXPART has been successfully used to identify long range transport of biomass burning emissions in many studies (e.g. Brioude

et al., 2007; Stohl et al., 2007; Lapina et al., 2008; Quennehen et al., 2011, 2012; Schmale et al., 2011; Cristofanelli et al., 2013). Biomass burning events were characterized as having a FLEXPART BC_{fire} tracer > 90th percentile ($\simeq 7\,pmol\,mol^{-1}$). In total, 13 events were observed between July 2008 and July 2010 ranging in duration between 12 and 252 h. Details regarding the start date, duration, mean plume age, FLEXPART tracer levels and trace gas levels for each event are shown in Table 3. A more conservative threshold was applied here than for the anthropogenic emissions in Sect. 3.2.1,consequently, the events identified had significant BB impacts but small anthropogenic signatures. Of these 13 events, 2 were identified as having potentially high anthropogenic signatures (BC_{anthro} > 75th percentile) and were most likely plumes of mixed anthropogenic and biomass burning emissions, 6 events were identified as having medium anthropogenic signatures (75th percentile > BC_{anthro} > 50th percentile) and the remaining 5 events were classified as having low anthropogenic signatures. The source contribution from FLEXPART shows that the majority of the BB events (9 out of 13) originated in North America, with the BB events originating in Europe all occurring in March 2009.

Analyses of O_3 and its precursors at Summit show that the mean enhancements for PAN, NO_x, NO_y, and C_2H_6 during the BB events identified by FLEXPART are highly variable (Table 3). Values ranged between -4.6 and $13.0\,nmol\,mol^{-1}$ for ΔO_3, -20.9 to $83.5\,pmol\,mol^{-1}$for ΔPAN, 1.8 to $22.6\,pmol\,mol^{-1}$for ΔNO_x, 11.8 to $135\,pmol\,mol^{-1}$ for ΔNO_y, and -11.3 to $113\,pmol\,mol^{-1}$ for ΔC_2H_6. Ethane levels were low during the summer in general, and there is a large gradient in NMHC with latitude (Blake et al., 2003), therefore, small or negative ΔC_2H_6 values are expected at Summit, even with the transport of air masses from the south.

The range of O_3 enhancements observed here are comparable to those by Thomas et al. (2013), who estimated ozone production of up to $3\,nmol\,mol^{-1}$ in aged BB plumes in the mid to upper-troposphere (peaking at 7 km) over Greenland. Our results suggest that in the lower troposphere the enhancement may even be greater. The largest BB event identified by FLEXPART was observed in August 2008 (event 3), when the BC_{fire} tracer indicated BB plumes impacted the site continuously from 3 August to 14 August, peaking

at $\sim 91\,\mathrm{pmol\,mol^{-1}}$, as a result of large wildfires in Canada. We find O_3 and its precursors were all positive during this period, with mean enhancements of 13.9, and 141 $\mathrm{pmol\,mol^{-1}}$ for ΔNO_x and ΔNO_y respectively. PAN data was not available during the main peak of the event, however, PAN from 6 August onwards was elevated above background levels, with a mean ΔPAN value of $83.5\,\mathrm{pmol\,mol^{-1}}$. A closer analysis of the measurements in Fig. 10 shows that O_3 was consistently high during the event with a mean enhancement of $10.5\,\mathrm{nmol\,mol^{-1}}$. The FLEXPART total column sensitivity shows that air masses were typically transported between 2500 and 3500 m.a.s.l to Summit. FLEXPART also indicates that anthropogenic pollution was present during this period, therefore, enhancements observed in the gas species may also be the result of anthropogenic pollution.

Enhanced PAN, NO_x, and NO_y were observed during two BB events on July 17 and 18 July 2009 (event 8 and 9). Plumes during both events were transported at lower altitudes ($\sim$1950-2900 m) than the BB plume in August 2008, and had low anthropogenic signatures. Mean ΔO_3 levels were 4.6 and 13.0 $\mathrm{nmol\,mol^{-1}}$ during event numbers 8 and 9, respectively, suggesting the BB emissions resulted in photochemical production of O_3 during transport to the site. Care must be taken when interpreting these results. All the BB plumes sampled during this study have long transport times from source region to the measurement site, with mean weighted plume ages for the events ranging between 9–18 days (median 14 days). These aged plumes will be well mixed with background air, therefore, separating the pollution impacts from background levels is challenging.

Aged plumes transported at higher altitudes have a higher probability of mixing with high ozone from stratospheric origin, which may contribute to the elevated O_3 levels that were observed. For example, during event 7, FLEXPART indicates that an aged plume (mean age $\sim$ 16 days) originating from Asia, was transported over the North Pole between $\sim$3000-4200 m.a.s.l. A similar transport pattern was observed during the POLARCAT campaign, during which a plume, originating from Asia, was lifted within a warm conveyor belt over the North Pole towards Greenland (Roiger et al., 2011). The plume was then transported into the lower stratosphere, resulting in a well mixed tropospheric-stratospheric air mass with high O_3 levels. The plume during event 7 was transported at lower altitudes, however,

mixing with air from stratospheric origin is not impossible and may be the cause of the O_3 (ΔO_3=10.7 nmol mol^{-1}) and PAN (ΔPAN=71.6 pmol mol^{-1}) levels observed.

BB plumes that are well mixed with background air can result in low precursor levels. In 2008 FLEXPART indicated that a BB event impacted the measurement site from 25–26 July (event 1). The total column sensitivity from the FLEXPART retroplume (see Fig. 11) shows that the air masses arriving at the site during this event originated from a region with BB sources over Canada and Alaska and were transported in the lower troposphere over the Arctic Ocean for $\sim$ 4 days before ascending to Summit. The mean enhancement for O_3 during this event was -4.6 nmol mol^{-1} and O_3 precursors have small enhancements. Similar results were observed in March 2009 (events 4, 5, 6), when ΔPAN values were low or negative and ΔO_3 levels were below 4 nmol mol^{-1}. During all 3 of these events, the air masses spent many days in the lower troposphere, over the Arctic ocean and the edge of the Greenland ice sheet, before ascending to Summit in 1–2 days. It is likely, during these events, the aged plumes were well mixed with marine air with low O_3 and precursor mixing ratios.

4 Summary

These analyses of NO_y, NO_x, PAN, NMHC, and O_3 from the high altitude GEOSummit Station in Greenland show that PAN is the dominant species of NO_y at the site year-round, with monthly mean contributions ranging from a minimum of 42 % in the summer months to 76 % in spring. However, the NO_y seasonal cycle does not follow that of PAN, due to significant contributions from NO_x in the summer, and odd NO_y species during both summer and winter. We hypothesize that HNO_3, HONO, and alkyl nitrates are the largest sources of odd NO_y in the summer months. During the winter, mean monthly odd NO_y levels reach over 100 pmol mol^{-1}. Approximately 1/3 of the odd NO_y is likely to be alkyl nitrates transported to the site. Previous studies have suggested that HONO, HNO_3, NO_3, N_2O_5, and HO_2NO_2 may also contribute to the wintertime NO_y levels.

Rapid changes in the origin of sampled air masses, from regions in Europe, North America, and the high latitude Arctic, result in a large variability in the measured species. Individual pollution events during November to March 2008/2009 and 2009/2010 show polluted air masses resulted in elevated ozone precursors above the background level with mean enhancements up to 334 pmol mol^{-1}, 295 pmol mol^{-1}, 88 pmol mol^{-1}, and 1119 pmol mol^{-1} for NO_y, PAN, NO_x, and ethane, respectively. Enhancement values for PAN and ethane during the second winter were higher, possibly as a result of the increase in the contribution of air masses from Europe in 2009-2010 compared to 2008-2009. FLEXPART BC tracers and retroplume simulations indicate that European sources dominated the anthropogenic emissions impacting the site in November–March, contributing up to 56 % of the anthropogenic BC tracer in 2009, and 69 % in 2010. During the two winter seasons, 16 of the 52 events identified had negative mean ΔO_3 levels. These events often coincided with the arrival of polluted air masses that were transported quickly to the site, in only a few days, or transported within the lower troposphere. The reduced O_3 within the plumes was likely due to the occurrence of O_3 titration and reduced mixing with the higher background O_3 at Summit. Enhanced O_3 levels were also observed during the winter pollution events. These were typically associated with transport up to $\sim$ 3000-4000 m.a.s.l, increasing the probability of mixing with O_3 rich air from stratospheric origin.

FLEXPART tracer simulations indicated that biomass burning emissions transported to Summit during the summer in 2008–2010 primarily originated from North America. Biomass burning plumes from Europe were only present during a short period in March 2009. During 2009 measurements were performed over a full summer period, however, BB impacts were low in summer 2009, compared to 2008 and 2010. In total, 13 plumes were identified, and only 5 with low anthropogenic signatures. During the events, O_3 and precursor levels were typically enhanced within the BB plumes with ΔO_3 levels up to 13.0 nmol mol^{-1} and ΔPAN, ΔNO_y, and ΔC_2H_6 levels enhanced by up to 83.5, 135 pmol mol^{-1} and 113 pmol mol^{-1}, respectively. The results presented here show that BB plumes may potentially impact the O_3 at Summit and the Arctic region in general, however, due to the long transport times and limited number of BB air masses transported to Summit during the measurement period, a

quantitative analysis of the impact of BB plumes on O_3 and O_3 precursor levels is difficult. Future studies, with coincident CO, O_3, and O_3 precursor measurements at Summit, would be valuable to determine enhancement ratios with respect to CO and evaluate the potential for ozone production in the region.

The data and results presented here show that the boundary layer at Summit is strongly impacted by both snowpack emissions and mixing of pollution plumes transported from North America and Europe. Anthropogenic emissions can impact the site year-round resulting in enhanced levels of NO_y in the boundary layer. Knowledge of pollution impacts over the Greenland ice sheet is important for modeling studies, in particular those that are focusing on snowpack-air exchange of gas species. Enhanced NO_y levels observed above the background during the events discussed here may have an important impact on snow photochemistry and the subsequent release of NO_x due to the uptake of NO_y species to the snowpack (Grannas et al., 2007, and references therein). Additionally, due to the stability of the Arctic free troposphere, the region is an effective reservoir for O_3 precursors. The high O_3 precursor mole fractions above background levels in spring and summer at Summit may have important implications for NO_x and O_3 in the mid-latitudes during southerly flow of air masses (Hamlin and Honrath, 2002).

The Supplement related to this article is available online at doi:10.5194/acpd-0-1-2015-supplement.

Acknowledgements. The authors acknowledge support for this project from the NASA ROSES program, grant number NNX07AR26G. A. Stohl was supported by the Norwegian Research Council in the framework of POLARCAT-Norway. Support for J.F. Burkhart was provided jointly under the Norwegian Research Council (project ES432275) and the U.S. National Science Foundation (NSF1023651). The authors would like to acknowledge Mike Dziobak at Michigan Tech for all his valuable work with the instrumentation and Brie Van Dam and Jacques Heuber from The University of Colorado, Boulder, assisting with the measurements. We would like to thank the 109th Air National Guard and the support staff and science technicians from CH2M Hill Polar Field Services for

their valuable assistance and the Danish Commission for Scientific Research for providing access to GEOSummit Station. The authors would also like to thank Jack Dibb and Meredith Hastings for sharing the HNO_3 and HONO data from Summit.

References

Alexander, B.,Savarino, J., Kreutz, K. J., and Thiemens, M. H.: Impact of preindustrial biomass-burning emissions on the oxidation pathways of tropospheric sulfur and nitrogen, J. Geophys. Res., 109, D08303, doi:10.1029/2003JD004218, 2004.

Alvarado, M. J., Logan, J. A., Mao, J., Apel, E., Riemer, D., Blake, D., Cohen, R. C., Min, K.-E., Perring, A. E., Browne, E. C., Wooldridge, P. J., Diskin, G. S., Sachse, G. W., Fuelberg, H., Sessions, W. R., Harrigan, D. L., Huey, G., Liao, J., Case-Hanks, A., Jimenez, J. L., Cubison, M. J., Vay, S. A., Weinheimer, A. J., Knapp, D. J., Montzka, D. D., Flocke, F. M., Pollack, I. B., Wennberg, P. O., Kurten, A., Crounse, J., Clair, J. M. St., Wisthaler, A., Mikoviny, T., Yantosca, R. M., Carouge, C. C., and Le Sager, P.: Nitrogen oxides and PAN in plumes from boreal fires during ARCTAS-B and their impact on ozone: an integrated analysis of aircraft and satellite observations, Atmos. Chem. Phys., 10, 9739–9760, doi:10.5194/acp-10-9739-2010, 2010.

Anderson, P. S. and Neff, W. D.: Boundary layer physics over snow and ice, Atmos. Chem. Phys., 8, 13, 3563–3582, 2008.

Atlas, E. L.,Ridley, B. A. and Cantrell, C.: The Tropospheric Ozone Production about the Spring Equinox (TOPSE) Experiment: Introduction, J. Geophys. Res., 108, 8353, doi:10.1029/2002JD003172, D4, 2003.

Barrie, L. A. and Bottenheim, J. W.: Sulphur and nitrogen pollution in the Arctic atmosphere, in: Pollution of The Arctic Atmosphere, edited by: Sturges, W., Elsevier Press, New York, 155–183, 1991.

Beine, H. J. and Krognes, T.: The seasonal cycle of peroxyacetyl nitrate (PAN) in the European Arctic, Atmos. Environ., 34, 933–940, doi:10.1016/S1352-2310(99)00288-5, 2000.

Beine, H. J., Jaffe, D. A., and Herring, J. A.: High-latitude springtime photochemistry, Part I: NO_x, PAN and Ozone Relationships, J. Atmos. Chem., 27, 127–153, 1997.

Beine, H. J., Honrath, R. E., Dominè, F., Simpson, W. R., and Fuentes, J. D.: NO_x during background and ozone depletion periods at Alert: Fluxes above the snow surface, J. Geophys.Res., 107, 4584, doi:10.1029/2002JD002082, 2002.

Beine, H. J., Dominè, F., Ianniello, A., Nardino, M., Allegrini, I., Teinilä, K., and Hillamo, R.: Fluxes of nitrates between snow surfaces and the atmosphere in the European high Arctic, Atmos. Chem. Phys., 3, 335–346, doi:10.5194/acp-3-335-2003, 2003.

Bian, H., Colarco, P. R., Chin, M., Chen, G., Rodriguez, J. M., Liang, Q., Blake, D., Chu, D. A., da Silva, A., Darmenov, A. S., Diskin, G., Fuelberg, H. E., Huey, G., Kondo, Y., Nielsen, J. E., Pan, X., Wisthaler, A.: Source attributions of pollution to the Western Arctic during the NASA ARCTAS field campaign Atmos. Chem. Phys., 13,4707–4721, doi:10.5194/acp-13-4707-2013, 2007.

Blake, N. J., Blake, D. R., Sive, B. C., Katzenstein, A., Meinardi, S., Wingenter, O. W., Atlas, E. L., Flocke, F., Ridley, B. A., and Sherwood Rowland, F.: The seasonal evolution of NMHCs and light alkyl nitrates at middle to high northern latitudes during TOPSE, J. Geophys. Res., 108, 8359, doi:10.1029/2001JD001467, 2003.

Bollinger, M. J., Sievers, R. E., Fahey, D. W., and Fehsenfeld, F. C.: Conversion of nitrogen dioxide, nitric acid, and n-propyl nitrate to nitroc oxide by gold-catalzed reduction with carbon monoxide, Anal. Chem., 55, 1980–1986, 1983.

Bottenheim, J. W., Sirois, A., Brice, K. A., and Gallant, A. J.: Five years of continuous observations of PAN and ozone, J. Geophys. Res., 99, 5333–5352, 1994.

Brioude, J., Cooper, O. R., Trainer, M., Ryerson, T. B., Holloway, J. S., Baynard, T., Peischl, J., Warneke, C., Neuman, J. A., De Gouw, J., Stohl, A., Eckhardt, S., Frost, G. J., McKeen, S. A., Hsie, E.-Y., Fehsenfeld, F. C., and Nédélec, P.: Mixing between a stratospheric intrusion and a biomass burning plume, Atmos. Chem. Phys., 7, 4229–4235, doi:10.5194/acp-7-4229-2007, 2007.

Browell, E. V., Hair, J. W., and Butler, C. F.: Ozone, aerosol, potential vorticity, and trace gas trends observed at high-latitudes over North America from February to May 2000, J. Geophys. Res., 108, 1–16, doi:10.1029/2001JD001390, 2003.

Chen, G., Davis, D., Crawford, J., Hutterli, L. M., Huey, L. G., Slusher, D., Mauldin, L., Eisele, F., Tanner, D., Dibb, J., Buhr, M., McConnell, J., Lefer, B., Shetter, R., Blake, D., Song, C. H., Lombardi, K., and Arnoldy, J.: A reassessment of {HOx} South Pole chemistry based on observations recorded during ISCAT 2000, Atmos. Environ., 38, 5451–5461, 2004.

Chen, G. Huey, L. G. Crawford, J. H., Olson, J. R., Hutterli,M . A., Sjostedt, S., Tanner, D., Dibb, J., Lefer, B., Blake, N., Davis, Douglas and Stohl A.: An assessment of the polar {HOx} photochemical budget based on 2003 Summit Greenland field observationsAtmos. Environ., 36, 7806–7820,doi:http://dx.doi.org/10.1016/j.atmosenv.2007.06.014, 2007.

Cohen, L., Helmig, D., Neff, W., Grachev, A. A. and Fairall, C. W.: Boundary-layer dynamics and its influence on atmospheric chemistry at Summit, Greenland, Atmos. Environ., 41, 24, 5044–5060, 2007.

Cristofanelli, P., Fierli, F., Marinoni, A., Calzolari, F., Duchi, R., Burkhart, J., Stohl, A., Maione, M., Arduini, J., and Bonasoni, P.: Influence of biomass burning and anthropogenic emissions on ozone, carbon monoxide and black carbon at the Mt. Cimone GAW-WMO global station (Italy, 2165 m a.s.l.), Atmos. Chem. Phys., 13, 15–30, doi:10.5194/acp-13-15-2013, 2013.

Cullen, N. J. and Steffen, K.:Unstable near-surface boundary conditions in summer on top of the Greenland Ice Sheet, Geophys. Res., Lett., 28, 23,4491–4493, 2001.

Dassau, T. M., Shepson, P. B., Bottenheim, J. W., and Ford, K. M.: Peroxyacetyl nitrate photochemistry and interactions with the Arctic surface, J. Geophys. Res., 109, D18302, doi:10.1029/2004JD004562, 2004.

Dibb, J. E., and Fahnestock, M.: Snow accumulation, surface height change, and firn densification at Summit, Greenland: Insights from 2 years of in situ observation, J. Geophys. Res., 109, D24113, doi:10.1029/2003JD004300, 2004.

Dibb, J. E., Talbot, R W., Robert, W., and Bergin, M. H.: Soluble acidic species in air and snow at Summit, Greenland, Geophys. Res. Lett., 21,1627–1630, 1994.

Dibb, J. E., Talbot, R W., Munger, J. W., Jacob, D. J., and Fan, S. M.: Air-snow exchange of HNO_3 and NO_y at Summit, Greenland, J. Geophys. Res., 103, 3475–3486, 1998.

Dibb, J. E., Arsenault, M., Peterson, M. C., and Honrath, R. E.: Fast nitrogen oxide photochemistry in Summit, Greenland snow, Atmos. Environ., 36, 2501–2511, doi:10.1016/S1352-2310(02)00130-9, 2002.

Dibb, J. E.Albert, M., Anastasio, C., Atlas, E., Beyersdorf, A. J., Blake, N. J., Blake, D. R., Bocquet, F., Burkhart, J. F., Chen, G., Cohen, L., Conway, T. J., Courville, Z., Frey, M. M., Friel, D. K., Galbavy, E. S., Hall, S., Hastings, M. G., Helmig, D., Huey, L. G., Hutterli, M. A., Jarvis, J. C., Lefer, B. L., Meinardi, S., Neff, W., Oltmans, S. J., Rowland, F. S., Sjostedt, S. J., Steig, E. J., Swanson, A., L., and Tanner, D. J.: An overview of air-snow exchange at Summit, Greenland: Recent experiments and findings, Atmos. Environ., 41, 24,4995 - 5006 doi:10.1016/j.atmosenv.2006.12.006, 2007.

Dominé, F. and Shepson, P. B.: Air-snow interactions and atmospheric chemistry, Science, 297, 1506–1510, doi:10.1126/science.1074610, 2002.

Emmons, L. K, Hess, P., Klonecki, A., Tie, X., Horowitz, L.,Lamarque, J. -F., Kinnison, D., Brasseur, G.,Atlas, E.,Browell, E., Cantrell, C., Eisele, F., Mauldin, R. L., Merrill, J., Ridley, B.,

and Shetter R.:Budget of tropospheric ozone during TOPSE from two chemical transport models,J. Geophys. Res.,108.,D8, 8372, doi:10.1029/2002JD002665, 2003.

Eneroth, K., Holmén, K., Berg, T., Schmidbauer, N., and Solberg, S.: Springtime depletion of tropospheric ozone, gaseous elemental mercury and non-methane hydrocarbons in the European Arctic, and its relation to atmospheric transport, Atmos. Environ., 41, 8511–8526, doi:10.1016/j.atmosenv.2007.07.008, 2007.

Fahey, D. W., Eubank, C. S., Hubler, G., and Fehsenfeld, F. C.: Evaluation of a catalytic reduction technique for the measurement of total reactive odd-nitrogen NO_y in the atmosphere, Atmos. Chem., 3, 435–468, 1985.

Fisher, J. A., Jacob, D. J., Purdy, M. T., Kopacz, M., Le Sager, P., Carouge, C., Holmes, C. D., Yantosca, R. M., Batchelor, R. L., Strong, K., Diskin, G. S., Fuelberg, H. E., Holloway, J. S., Hyer, E. J., McMillan, W. W., Warner, J., Streets, D. G., Zhang, Q., Wang, Y., Wu, S.: Source attribution and interannual variability of Arctic pollution in spring constrained by aircraft (ARCTAS, ARCPAC) and satellite (AIRS) observations of carbon monoxide, Atmos. Chem. Phys., 10, 977–996, doi:10.5194/acp-10-977-2010, 2010.

Ford, K. M., Campbell, B. M., Bertman, S. B., Honrath, R. E., Peterson, M. C., and Dibb, J. E.: Studies of Peroxyacetyl nitrate (PAN) and its interaction with the snowpack at Summit, Greenland, J. Geophys. Res., 107, 1–10, 2002.

Fuhrer, K., and. Legrand, M.: Continental biogenic species in the Greenland Ice Core Project ice core: Tracing back the biomass history of the North American continent, J. Geophys. Res., 102(C12), 26,735–26,745, doi:10.1029/97JC01299, 1997.

Giglio, L., Descloitres, J., Justice, C. O., and Kaufman, Y.: An enhanced contextual fire detection algorithm for MODIS, Remote Sens. Environ., 87, 273–282, 2003.

Gilman, J. B. B., Burkhart, J. F. J. F., Lerner, B. M., Williams, E. J., Kuster, W. C., Goldan, P. D., Murphy, P. C., Warneke, C., Fowler, C., Montzka, S. A., Miller, B. R., Miller, L., Oltmans, S. J., Ryerson, T. B., Cooper, O. R., Stohl, A., and de Gouw, J. A.: Ozone variability and halogen oxidation within the Arctic and sub-Arctic springtime boundary layer, Atmos. Chem. Phys., 10, 15885–15919, doi:10.5194/acpd-10-15885-2010, 2010.

Grannas, A. M., Jones, A. E., Dibb, J., Ammann, M., Anastasio, C., Beine, H. J., Bergin, M., Bottenheim, J., Boxe, C. S., Carver, G., Chen, G., Crawford, J. H., Dominé, F., Frey, M. M., Guzmán, M. I., Heard, D. E., Helmig, D., Hoffmann, M. R., Honrath, R. E., Huey, L. G., Hutterli, M., Jacobi, H. W., Klán, P., Lefer, B., McConnell, J., Plane, J., Sander, R., Savarino, J., Shepson, P. B., Simpson, W. R., Sodeau, J. R., von Glasow, R., Weller, R., Wolff, E. W., and Zhu, T.: An overview of

snow photochemistry: evidence, mechanisms and impacts, Atmos. Chem. Phys., 7, 4329–4373, doi:10.5194/acp-7-4329-2007, 2007.

Hamlin, A. and Honrath, R.: A modeling study of the impact of winter-spring arctic outflow on the NO_x and O_3 budgets of the North Atlantic troposphere, J. Geophys. Res., 107, 1–46, doi:10.1029/2001JD000453, 2002.

Helmig D., Boulter, J., David D., Birks J. W., Cullen N. J., Steffen K., Johnson B. J., and Oltmans S. J.: Ozone and meteorological boundary-layer conditions at Summit, Greenland, during 3–21 June 2000, Atmos. Environ., 36, 15, 2595–2608, 2002.

Helmig, D., Oltmans, S. J., Carlson, D., Lamarque, J.-F., Jones, A., Labuschagne, C., Anlauf, K., and Hayden, K.: A review of surface ozone in the polar regions, Atmos. Environ., 41, 5138–5161, doi:10.1016/j.atmosenv.2006.09.053, 2007a.

Helmig, D., Oltmans, S. J., Morse, T. O., and Dibb, J. E.: What is causing high ozone at Summit, Greenland?, Atmos. Environ., 41, 5031–5043, doi:10.1016/j.atmosenv.2006.05.084, 2007b.

Helmig, D., Tanner, D. M., Honrath, R. E., Owen, R. C., and Parrish, D. D.: Nonmethane hydrocarbons at Pico Mountain, Azores: 1. Oxidation chemistry in the North Atlantic region, J. Geophys. Res., 113, D20S91, doi:10.1029/2007JD008930, 2008.

Helmig, D., Stephens, C., Caramore, J., and Hueber, J.: Seasonal behavior of non-methane hydrocarbons in the firn air at Summit, Greenland, Atmos. Environ., 85, 234–246, doi:10.1016/j.atmosenv.2013.11.021, 2014.

Hirdman, D., Sodemann, H., Eckhardt, S., Burkhart, J. F., Jefferson, A., Mefford, T., Quinn, P. K., Sharma, S., Ström, J., and Stohl, A.: Source identification of short-lived air pollutants in the Arctic using statistical analysis of measurement data and particle dispersion model output, Atmos. Chem. Phys., 10, 669–693, doi:10.5194/acp-10-669-2010, 2010.

Honrath, R. E. and Jaffe, D. A.: The seasonal cycle of nitrogen oxides in the Arctic troposphere at Barrow, Alaska, J. Geophys. Res., 97, 20615, doi:10.1029/92JD02081, 1992.

Honrath, R., Hamlin, A., and Merrill, J.: Transport of ozone precursors from the Arctic troposphere to the North Atlantic region, J. Geophys. Res., 101, 29335–29351, 1996.

Honrath, R., Peterson, M., Guo, S., Dibb, J. E., Shepson, P. B., and Campbell, B.: Evidence of NO_x production within or upon ice particles in the Greenland snowpack, Geophys. Res. Lett., 26, 695–698, 1999.

Honrath, R. E., Guo, S., and Peterson, M. C.: Photochemical production of gas phase NO from ice crystal NO_3^-, J. Geophys. Res., 105, 24183–24190, 2000a.

Honrath, R. E., Peterson, M. C., Dziobak, M. P., Dibb, J. E., Arsenault, M. A., and Green, S. A.: Release of NO_x from sunlight-irradiated midlatitude snow, Geophys. Res. Lett., 27, 2237–2240, doi:10.1029/1999GL011286, 2000b.

Honrath, R. E., Lu, Y., and Peterson, M. C.: Vertical fluxes of NO_x, HONO, and HNO_3 above the snowpack at Summit, Greenland, Atmos. Environ., 36, 2629–2640, 2002.

Honrath, R. E., Helmig, D., Owen, R. C., Parrish, D. D., and Tanner, D. M.: Nonmethane hydrocarbons at Pico Mountain, Azores: 2. Event-specific analyses of the impacts of mixing and photochemistry on hydrocarbon ratios, J. Geophys. Res., 113, D20S92, doi:10.1029/2008JD009832, 2008.

Hornbrook, R. S., Blake, D. R., Diskin, G. S., Fried, A., Fuelberg, H. E., Meinardi, S., Mikoviny, T., Richter, D., Sachse, G. W., Vay, S. A., Walega, J., Weibring, P., Weinheimer, A. J., Wiedinmyer, C., Wisthaler, A., Hills, A., Riemer, D. D., and Apel, E. C.: Observations of nonmethane organic compounds during ARCTAS – Part 1: Biomass burning emissions and plume enhancements, Atmos. Chem. Phys., 11, 11103–11130, doi:10.5194/acp-11-11103-2011, 2011.

Jobson, B., Wu, Z., Niki, H., and Barrie, L. A.: Seasonal trends of isoprene, C_2–C_5 alkanes, and acetylene at a remote boreal site in Canada, J. Geophys. Res., 99, 1589–1599, 1994.

Jones, A. E., Brough, N., Anderson, P. S., and Wolff, E. W.: HO_2NO_2 and HNO_3 in the coastal Antarctic winter night: a "lab-in-the-field" experiment, Atmos. Chem. Phys. Discuss., 14, doi:10.5194/acpd-14-12771-2014, 2014.

Justice, C. O., Giglio, L., Korontzi, S., Owens, J., Morisette, J. T., Roy, D., Descloitres, J., Alleaume, S., Petitcolin, F., and Kaufman, Y.: The MODIS fire products, Remote Sens. Environ., 83, 244–262, 2002.

Kahl, J. D. W., Martinez, D. A., Kuhns, H., Davidson, C. I., Jaffrezo, J. L., and Harris, J. M.: Air mass trajectories to Summit, Greenland: a 44-year climatology and some episodic events, J. Geophys. Res.-Oceans, 102, 26861–26875,doi:10.1029/97jc00296, 1997.

Karbiwnyk, C. M., Mills, C. S., Helmig, D., and Birks, J. W.: Use of chloroflurocarbons as internal standards for the measurement of atmospheric non-methane volatile organic compounds sampled onto solid adsorbent cartridges, Environ. Sci. Technol., 37, 1002–7, 2003.

Kley, D. and Mcfarland, M.: Chemiluminescence detector for NO and NO_2, Atmospheric Measurement Techniques, 12, 63–69, 1980.

Klonecki, A., Hess, P., Emmons, L., Smith, L., Orlando, J, and Blake, D.: Seasonal changes in the transport of pollutants into the Arctic troposphere-model study, J. Geophys. Res., 108, 8367, doi:10.1029/2002JD002199, 2003.

Lamarque, J.-F. and Hess, P. G.: Model analysis of the temporal and geographical origin of the CO distribution during the TOPSE campaign, J. Geophys. Res.,108, 8369,doi:10.1029/2002JD002077, 2003.

Lapina, K., Honrath, R. E., Owen, R. C., Val Martín, M., Hyer, E. J., and Fialho, P.: Late summer changes in burning conditions in the boreal regions and their implications for NO_x and CO emissions from boreal fires, J. Geophys. Res., 113, D11304, doi:10.1029/2007JD009421, 2008.

Law, K. S. and Stohl, A.: Arctic air pollution: origins and impacts, Science, 315, 1537–1540, doi:10.1126/science.1137695, 2007.

Law, K. S., Stohl, A., Quinn, P. K., Brock, C., Burkhart, J., Paris, J-D., Ancellet, G., Singh, H. B., Roiger, A., Schlager, H., Dibb, J., Jacob, D. J., Arnold, S. R., Pelon, J., Thomas, J. L.: Arctic Air Pollution: New Insights From POLARCAT-IPY, Bulletin of the American Meteorological Society, 315,0003-0007, doi:10.1175/BAMS-D-13-00017.1, 2014.

Legrand, M., and de Angelis, M.: Light carboxylic acids in Greenland ice: A record of past forest fires and vegetation emissions from the boreal zone, J. Geophys. Res., 101(D2), 4129–4145, doi:10.1029/95JD03296, 1996.

Liang, Q., Rodriguez, J. M., Douglass, A. R., Crawford, J. H., Olson, J. R., Apel, E., Bian, H., Blake, D. R., Brune, W., Chin, M., Colarco, P. R., da Silva, A., Diskin, G. S., Duncan, B. N., Huey, L. G., Knapp, D. J., Montzka, D. D., Nielsen, J. E., Pawson, S., Riemer, D. D., Weinheimer, A. J., and Wisthaler, A.: Reactive nitrogen, ozone and ozone production in the Arctic troposphere and the impact of stratosphere-troposphere exchange, Atmos. Chem. Phys., 11, 13181–13199, doi:10.5194/acp-11-13181-2011, 2011.

Liao, W., Case, A. T., Mastromarino, J., Tan, D. and Dibb, J. E.: Observations of HONO by laser-induced fluorescence at the South Pole during ANTCI 2003, Geophys. Res. Lett., 33, L09810, doi:10.1029/2005GL025470, 2006.

Liao, J., Huey, L. G., Tanner, D. J., Brough, N., Brooks, S., Dibb, J. E., Stutz, J., Thomas, J. L., Lefer, B., Haman, C. and Gorham, K.: Observations of hydroxyl and peroxy radicals and the impact of BrO at Summit, Greenland in 2007 and 2008, Atmos. Chem. Phys., 11, 8577–8591, doi:10.5194/acp-11-8577-2011, 2011.

Monks, P. S.: A review of the observations and origins of the spring ozone maximum, Atmos. Environ., 34, 3545–3561, doi:10.1016/S1352-2310(00)00129-1, 2000.

Munger, J. W., Jacob, D. J., and Fan, S. M., Colman, A. S., and Dibb, J. E.: Concentrations and snow-atmosphere fluxes of reactive nitrogen at Summit, Greenland, J. Geophys. Res., 104, 13,721–13,734, 1999.

Murray, K., Kramer L., Doskey, P., Ganzeveld, L., Seok, B., Van Dam, B., and Helmig, D.: Dynamics of ozone and nitrogen oxides at Summit, Greenland: II. Model presentation and chemical dynamics during a high ozone event, in preparation, 2014.

Muthuramu, K., Shepson, P. B., Bottenheim, J. W., Jobson, B. T., Niki, H., and Anlauf, K. G.: Relationships between organic nitrates and surface ozone destruction during Polar Sunrise Experiment 1992, J. Geophys. Res., 99, 13,721–13,734, 1994.

Parrish, D. D., Dunlea, E. J., Atlas, E. L., Schauffler, S., Donnelly, S., Stoud, V., Goldstein, A. H., Millet, D. B., McKay, M., Jaffe, D. A., Price, H. U., Hess, P. G., Flocke, F., and Roberts, J. M: Changes in the photochemical environment of the temperate North Pacific troposphere in response to increased Asian emissions, J. Geophys. Res., 109, D23S18, doi:10.1029/2004JD004978, 2004.

Penkett, S., Blake, N., Lightman, P., Marsh, A., Anwyl, P., and Butcher, G.: The seasonal variation of nonmethane hydrocarbons in the free troposphere over the North Atlantic Ocean: possible evidence for extensive reaction of hydrocarbons, J. Geophys. Res., 98, 2865–2885, 1993.

Peterson, M. C. and Honrath, R. E.: NO_x and NO_y over the northwestern North Atlantic: measurements and measurement accuray, J. Geophys. Res., 103, 13489–13503, 1999.

Petropavlovskikh, I. and Oltmans, S. J.: Tropospheric Ozone Measurements, 1973–2011, Version: 2012-07-10, NOAA, ftp://aftp.cmdl.noaa.gov/data/ozwv/SurfaceOzone/ (last access: 24 March 2013), 2012.

Pollack, I. B., Lerner, B. M., and Ryerson, T. B.: Evaluation of ultraviolet light-emitting diodes for detection of atmospheric NO_2 by photolysis – chemiluminescence, J. Atmos. Chem., 65, 111–125, doi:10.1007/s10874-011-9184-3, 2011.

Quennehen, B., Schwarzenboeck, A., Schmale, J., Schneider, J., Sodemann, H., Stohl, A., Ancellet, G., Crumeyrolle, S., and Law, K. S.: Physical and chemical properties of pollution aerosol particles transported from North America to Greenland as measured during the POLARCAT summer campaign, Atmos. Chem. Phys., 11, 10947–10963, doi:10.5194/acp-11-10947-2011, 2011.

Quennehen, B., Schwarzenboeck, A., Matsuki, A., Burkhart, J. F., Stohl, A., Ancellet, G., and Law, K. S.: Anthropogenic and forest fire pollution aerosol transported to the Arctic: observations from the POLARCAT-France spring campaign, Atmos. Chem. Phys., 12, 6437–6454, doi:10.5194/acp-12-6437-2012, 2012.

Quinn, P. K., Bates, T. S., Baum, E., Doubleday, N., Fiore, A. M., Flanner, M., Fridlind, A., Garrett, T. J., Koch, D., Menon, S., Shindell, D., Stohl, A., and Warren, S. G.: Short-lived pollutants in the Arctic: their climate impact and possible mitigation strategies, Atmos. Chem. Phys., 8,doi:10.5194/acp-8-1723-2008, 2008.

Ridley, B. A. and Grahek, F.: A small, low flow, high sensitivity reaction vessel for NO chemiluminescence detectors, American Meteorlogical Society, 7, 307–311, 1990.

Roiger, A., Aufmhoff, H., Stock, P., Arnold, F., and Schlager, H.: An aircraft-borne chemical ionization – ion trap mass spectrometer (CI-ITMS) for fast PAN and PPN measurements, Atmos. Meas. Tech., 4, 173–188, doi:10.5194/amt-4-173-2011, 2011.

Sander, S. P., Abbatt, J. Barker, J. R., Burkholder, J. B., Friedl, R R., Golden, D. M., Huie, R. E., Kolb, C. E., Kurylo, M. J., Moortgat, G. K., Orkin V. L., and Wine, P. H.: Chemical Kinetics and Photochemical Data for Use in Atmospheric Studies, Evaluation No. 17, JPL Publication 10-6, Jet Propulsion Laboratory, Pasadena, 2011, 2013, http://jpldataeval.jpl.nasa.gov.

Schmale, J., Schneider, J., Ancellet, G., Quennehen, B., Stohl, A., Sodemann, H., Burkhart, J. F., Hamburger, T., Arnold, S. R., Schwarzenboeck, A., Borrmann, S., and Law, K. S.: Source identification and airborne chemical characterisation of aerosol pollution from long-range transport over Greenland during POLARCAT summer campaign 2008, Atmos. Chem. Phys., 11, 10097–10123, doi:10.5194/acp-11-10097-2011, 2011.

Shindell, D.: Local and remote contributions to Arctic warming, Geophys. Res. Lett., 34, L14704, doi:10.1029/2007GL030221, 2007.

Shindell, D., Faluvegi, G., Lacis, A., Hansen, J., Ruedy, R., and Aguilar, E.: Role of tropospheric ozone increases in 20th-century climate change, J. Geophys. Res., 111, D08302, doi:10.1029/2005JD006348, 2006.

Shindell, D. T., Chin, M., Dentener, F., Doherty, R. M., Faluvegi, G., Fiore, A. M., Hess, P., Koch, D. M., MacKenzie, I. A., Sanderson, M. G., Schultz, M. G., Schulz, M., Stevenson, D. S., Teich, H., Textor, C., Wild, O., Bergmann, D. J., Bey, I., Bian, H., Cuvelier, C., Duncan, B. N., Folberth, G., Horowitz, L. W., Jonson, J., Kaminski, J. W., Marmer, E., Park, R., Pringle, K. J., Schroeder, S., Szopa, S., Takemura, T., Zeng, G., Keating, T. J., and Zuber, A.: A multi-model assessment of pollution transport to the Arctic, Atmos. Chem. Phys., 8, 5353–5372, doi:10.5194/acp-8-5353-2008, 2008.

Shindell, D., Kuylenstierna, J. C. I., Vignati, E., van Dingenen, R., Amann, M., Klimont, Z., Anenberg, S. C., Muller, N., Janssens-Maenhout, G., Raes, F., Schwartz, J., Faluvegi, G., Pozzoli, L., Kupiainen, K., Höglund-Isaksson, L., Emberson, L., Streets, D., Ramanathan, V., Hicks, K., Oanh, N. T. K., Milly, G., Williams, M., Demkine, V., and Fowler D.: Simultaneously mitigating near-term climate change and improving human health and food security. Science, 335, 183-189,doi:10.1126/science.1210026, 2012.

Singh, H., Anderson, B., Brune, W., Cai, C., Cohen, R., Crawford, J., Cubison, M., Czech, E., Emmons, L., and Fuelberg, H.: Pollution influences on atmospheric composition and chemistry at high northern latitudes: boreal and California forest fire emissions, Atmos. Environ., 44, 4553–4564, doi:10.1016/j.atmosenv.2010.08.026, 2010.

Solberg, S., Krognes, T., Stordal, F., Hov, Ø., Beine, H. J., Jaffe, D. A., Clemitshaw, K. C., and Penkett, S. A.: Reactive nitrogen compounds at Spitsbergen in the Norwegian Arctic, J. Atmos. Chem., 28, 209–225, 1997.

Stohl, A.: Characteristics of atmospheric transport into the Arctic troposphere, J. Geophys. Res., 111, D11306, doi:10.1029/2005JD006888, 2006.

Stohl, A., Forster, C., Eckhardt, S., Spichtinger, N., Huntrieser, H., Heland, J., Schlager, H., Wilhelm, S., Arnold, F., and Cooper, O.: A backward modeling study of intercontinental pollution transport using aircraft measurements, J. Geophys. Res., 108, 4370, doi:10.1029/2002JD002862, 2003.

Stohl, A., Forster, C., Frank, A., Seibert, P., and Wotawa, G.: Technical note: The Lagrangian particle dispersion model FLEXPART version 6.2, Atmos. Chem. Phys., 5, 2461–2474, doi:10.5194/acp-5-2461-2005, 2005.

Stohl, A., Andrews, E., Burkhart, J. F., Forster, C., Herber, A., Hoch, S. W., Kowal, D., Lunder, C., Mefford, T., Ogren, J. A., Sharma, S., Spichtinger, N., Stebel, K., Stone, R., Ström, J., Tørseth, K., Wehrli, C., and Yttri, K. E.: Pan-Arctic enhancements of light absorbing aerosol concentrations due to North American boreal forest fires during summer 2004, J. Geophys. Res., 111, D22214, doi:10.1029/2006JD007216, 2006.

Stohl, A., Berg, T., Burkhart, J. F., Fjæraa, A. M., Forster, C., Herber, A., Hov, Ø., Lunder, C., McMillan, W. W., Oltmans, S., Shiobara, M., Simpson, D., Solberg, S., Stebel, K., Ström, J., Tørseth, K., Treffeisen, R., Virkkunen, K., and Yttri, K. E.: Arctic smoke – record high air pollution levels in the European Arctic due to agricultural fires in Eastern Europe in spring 2006, Atmos. Chem. Phys., 7, 511–534, doi:10.5194/acp-7-511-2007, 2007.

Stohl, A., Klimont, Z., Eckhardt, S., Kupiainen, K., Shevchenko, V. P., Kopeikin, V. M., and Novigatsky, A. N.: Black carbon in the Arctic: the underestimated role of gas flaring and residential combustion emissions, Atmos. Chem. Phys., 13, 8833–8855, doi:10.5194/acp-13-8833-2013, 2013.

Stroud, C., Madronich, S., Atlas, E., Ridley, B., Flocke, F., Weinheimer, A., Talbot, B., Fried, A., Wert, B., Shetter, R., Lefer, B., Coffey, M., Heikes, B., and Blake, D.: Photochemistry in the arctic

free troposphere: NO_x budget and the role of odd nitrogen reservoir recycling, Atmos. Environ., 37, 3351–3364, doi:10.1016/S1352-2310(03)00353-4, 2003.

Swanson, A. L., Blake, N. J., Atlas, E., Flocke, F., Blake, D. R., and Sherwood Rowland, F.: Seasonal variations of C_2–C_4 nonmethane hydrocarbons and C_1–C_4 alkyl nitrates at the Summit research station in Greenland, J. Geophys. Res., 108, 4065, doi:10.1029/2001JD001445, 2003.

Tanner, D., Helmig, D., Hueber, J., and Goldan, P.: Gas chromatography system for the automated, unattended, and cryogen-free monitoring of C_2 to C_6 non-methane hydrocarbons in the remote troposphere, J. Chromatogr. A, 1111, 76–88, doi:10.1016/j.chroma.2006.01.100, 2006.

Thomas, J. L., Stutz, J., Lefer, B., Huey, L. G., Toyota, K., Dibb, J. E., and von Glasow, R.: Modeling chemistry in and above snow at Summit, Greenland – Part 1: Model description and results, Atmos. Chem. Phys., 11, 4899–4914, doi:10.5194/acp-11-4899-2011, 2011.

Thomas, J. L., Raut, J.-C., Law, K. S., Marelle, L., Ancellet, G., Ravetta, F., Fast, J. D., Pfister, G., Emmons, L. K., Diskin, G. S., Weinheimer, A., Roiger, A., and Schlager, H.: Pollution transport from North America to Greenland during summer 2008, Atmos. Chem. Phys., 13, 3825–3848, doi:10.5194/acp-13-3825-2013, 2013.

Ulrich, T., Ammann, M., Leutwyler, S., and Bartels-Rausch, T.: The adsorption of peroxynitric acid on ice between 230 K and 253 K, Atmos. Chem. Phys., 12, 1833–1845, doi:10.5194/acp-12-1833-2012, 2012.

UNEP: Integrated Assessment of Black Carbon and Tropospheric Ozone,2011, http://www.unep.org/dewa/Portals/67/pdf/BlackCarbon_report.pdf

Val Martín, M., Honrath, R. E., Owen, R. C., Pfister, G., Fialho, P., and Barata, F.: Significant enhancements of nitrogen oxides, black carbon, and ozone in the North Atlantic lower free troposphere resulting from North American boreal wildfires, J. Geophys. Res., 111, D23S60, doi:10.1029/2006JD007530, 2006.

Van Dam, B., Helmig, D., Neff, W. and Kramer, L.: Evaluation of Boundary Layer Depth Estimates at Summit Station, Greenland, Journal of Applied Meteorology and Climatology, 52, 10, 2356–2362, 2013.

Villena, G., Bejan, I., Kurtenbach, R., Wiesen, P., and Kleffmann, J.: Interferences of commercial NO_2 instruments in the urban atmosphere and in a smog chamber, Atmos. Meas. Tech., 5, 149–159, doi:10.5194/amt-5-149-2012, 2012.

Walker, T. W., Martin, R. V., van Donkelaar, A., Leaitch, W. R., MacDonald, A. M., Anlauf, K. G., Cohen, R. C., Bertram, T. H., Huey, L. G., Avery, M. A., Weinheimer, A. J., Flocke, F. M., Tarasick, D. W., Thompson, A. M., Streets, D. G., and Liu, X.: Trans-Pacific transport of reactive nitro-

gen and ozone to Canada during spring, Atmos. Chem. Phys., 10, 8353–8372, doi:10.5194/acp-10-8353-2010, 2010.

Walker, T. W., Jones, D. B. A., Parrington, M., Henze, D. K., Murray, L. T., Bottenheim, J. W., Anlauf, K., Worden, J. R., Bowman, K. W., Shim, C., Singh, K., Kopacz, M., Tarasick, D. W., Davies, J., von der Gathen, P., Thompson, A. M., and Carouge, C. C.: Impacts of midlatitude precursor emissions and local photochemistry on ozone abundances in the Arctic, J. Geophys. Res., 117, D01305, doi:10.1029/2011JD016370, 2012.

Weller, R., Minikin, A., König-Langlo, G., Schrems, O., Jones, A. E., Wolff, E. W., and Anderson, P. S.:Investigating possible causes of the observed diurnal variability in Antarctic NO_y, Geophys. Res. Lett.,26,18, doi:10.1029/1999GL900608, 1999.

Wespes, C., Emmons, L., Edwards, D. P., Hannigan, J., Hurtmans, D., Saunois, M., Coheur, P.-F., Clerbaux, C., Coffey, M. T., Batchelor, R. L., Lindenmaier, R., Strong, K., Weinheimer, A. J., Nowak, J. B., Ryerson, T. B., Crounse, J. D., and Wennberg, P. O.: Analysis of ozone and nitric acid in spring and summer Arctic pollution using aircraft, ground-based, satellite observations and MOZART-4 model: source attribution and partitioning, Atmos. Chem. Phys., 12, 237–259, doi:10.5194/acp-12-237-2012, 2012.

Whitlow, S., Mayewski, P. A.Dibb, J. E. Holdsworth, G., and Twickler, M.: An ice-core-based record of biomass burning in the Arctic and Subarctic, 1750–1980,Tellus, Ser. B, 46(3), 234–242, doi:10.1034/j.1600-0889.1994.t01-2-00006.x, 1994

Wofsy, S., Sachse, G., Gregory, G., Blake, D. R., Bradshaw, J. D., Sandholm, S. T., Singh, H., Barrick, J. A., Harriss, R. C., Talbot, R. W., Shipham, M. A., Browell, E. V., Jacob, D. J., and Logan, J. A.: Atmospheric chemistry in the Arctic and Subarctic: Influence of natural fires, industrial emissions, and stratospheric inputs, J. Geophys. Res., 97, 16731—16746, 1992.

Worthy, D., Trivett, N., Hopper, J. F., Bottenheim, J. W., and Levin, I.: Analysis of long range transport events at Alert, Northwest Territories, during the Polar Sunrise Experiment, J. Geophys. Res., 25329–25344, 99, 1994.

Yang, J., Honrath, R. E., Peterson, M. C., Dibb, J. E., Sumner, A. L., Shepson, P. B., Frey, M., Jacobi, H. -W., Swanson, A., and Blake, N.: Impacts of snowpack emissions on deduced levels of OH and peroxy radicals at Summit, Greenland, Atmos. Environ.,36,15,2523–2534, 2002.

Table 1. Monthly statistics for NO_x, NO_y, PAN, O_3 and the NO_y budget measured at Summit from 2008–2010.

Year	Month	NO_x (pmol mol^{-1}) Mean ± SD	NO_y (pmol mol^{-1}) Mean ± SD	PAN (pmol mol^{-1}) Mean ± SD	O_3 (pmol mol^{-1}) Mean ± SD	NO_x/NO_y[a] % Mean ± SD	PAN/NO_y[a] % Mean ± SD
2008	7	21 ± 18	133 ± 47	59 ± 27	46 ± 5	15 ± 7	42 ± 14
	8	17 ± 9	148 ± 66	79 ± 53	45 ± 7	13 ± 5	49 ± 17
	9	10 ± 7	94 ± 42	52 ± 31	39 ± 5	9 ± 7	51 ± 13
	10	2 ± 10	126 ± 57	81 ± 48	39 ± 4	1 ± 6	58 ± 19
	11	4 ± 16	165 ± 35	101 ± 22	40 ± 4	0 ± 5	58 ± 10
	12	−−	−−	88 ± 27	40 ± 2	−−	−−
2009	1	−−	−−	84 ± 20	44 ± 3	−−	−−
	2	−−	−−	106 ± 44	48 ± 4	−−	−−
	3	2 ± 11	288 ± 36	181 ± 77	49 ± 3	0 ± 4	56 ± 3
	4	19 ± 18	285 ± 77	217 ± 65	55 ± 6	7 ± 5	76 ± 11
	5	26 ± 19	242 ± 64	170 ± 41	56 ± 7	11 ± 7	72 ± 10
	6	19 ± 15	150 ± 43	94 ± 31	49 ± 8	13 ± 8	63 ± 12
	7	14 ± 18	123 ± 55	63 ± 26	43 ± 6	11 ± 12	51 ± 15
	8	15 ± 13	143 ± 41	94 ± 29	42 ± 4	10 ± 8	64 ± 10
	9	10 ± 13	114 ± 45	84 ± 33	40 ± 6	9 ± 8	72 ± 12
	10	6 ± 8	140 ± 43	95 ± 32	40 ± 5	5 ± 7	70 ± 9
	11	3 ± 7	184 ± 40	130 ± 36	42 ± 3	1 ± 3	65 ± 7
	12	4 ± 14	184 ± 55	119 ± 42	45 ± 3	1 ± 5	66 ± 16
2010	1	14 ± 25	181 ± 59	110 ± 41	47 ± 3	3 ± 4	55 ± 10
	2	5 ± 10	241 ± 89	125 ± 63	48 ± 3	2 ± 4	50 ± 12
	3	10 ± 10	244 ± 66	175 ± 73	51 ± 4	4 ± 4	73 ± 20
	4	25 ± 17	352 ± 102	273 ± 100	52 ± 6	7 ± 4	72 ± 11
	5	16 ± 18	230 ± 67	−−	52 ± 6	−−	−−
	6	20 ± 12	188 ± 63	−−	47 ± 7	−−	−−
	7	21 ± 11	231 ± 52	−−	50 ± 5	−−	−−

[a] PAN/NO_y and NO_x/NO_y ratios determined using coincident measurements only.

Table 2. Monthly statistics for NMHC measured at Summit from 2008–2010.

Year	Month	Ethane (pmol mol^{-1}) Mean ± SD	Propane (pmol mol^{-1}) Mean ± SD	i-Butane (pmol mol^{-1}) Mean ± SD	n-Butane (pmol mol^{-1}) Mean ± SD	i-Pentane (pmol mol^{-1}) Mean ± SD	n-Pentane (pmol mol^{-1}) Mean ± SD
2008	7	617 ± 37	46 ± 18	7 ± 7	8 ± 7	11 ± 9	−−
	8	593 ± 0	89 ± 0	10 ± 0	19 ± 0	10 ± 0	−−
	9	741 ± 70	151 ± 9	37 ± 12	68 ± 21	10 ± 5	8 ± 5
	10	952 ± 243	293 ± 146	47 ± 24	100 ± 49	31 ± 23	22 ± 15
	11	1308 ± 194	502 ± 138	89 ± 35	164 ± 57	51 ± 24	37 ± 18
	12	1574 ± 115	684 ± 85	129 ± 23	243 ± 49	79 ± 21	57 ± 13
2009	1	1884 ± 169	887 ± 118	182 ± 30	343 ± 52	130 ± 27	100 ± 19
	2	1846 ± 147	774 ± 107	139 ± 28	259 ± 51	87 ± 24	68 ± 19
	3	2100 ± 151	822 ± 116	136 ± 29	246 ± 56	75 ± 25	59 ± 18
	4	1779 ± 121	462 ± 91	54 ± 15	90 ± 27	20 ± 8	17 ± 7
	5	1380 ± 187	205 ± 84	17 ± 13	29 ± 18	5 ± 4	5 ± 4
	6	877 ± 98	61 ± 27	3 ± 3	6 ± 5	2 ± 1	2 ± 1
	7	617 ± 47	54 ± 22	6 ± 5	9 ± 6	3 ± 3	3 ± 2
	8	633 ± 65	73 ± 19	6 ± 4	13 ± 7	3 ± 2	3 ± 2
	9	710 ± 44	122 ± 36	15 ± 10	29 ± 18	8 ± 8	9 ± 7
	10	902 ± 113	259 ± 75	43 ± 16	80 ± 31	28 ± 13	24 ± 11
	11	1253 ± 125	482 ± 87	86 ± 20	162 ± 36	62 ± 20	52 ± 17
	12	1459 ± 238	623 ± 182	116 ± 45	220 ± 85	79 ± 35	66 ± 30
2010	1	1707 ± 340	714 ± 208	131 ± 45	245 ± 88	75 ± 33	61 ± 27
	2	1769 ± 323	697 ± 209	128 ± 51	229 ± 93	63 ± 32	53 ± 27
	3	1835 ± 174	619 ± 164	98 ± 43	181 ± 80	42 ± 25	34 ± 21
	4	1785 ± 381	530 ± 276	77 ± 62	138 ± 119	33 ± 34	27 ± 28
	5	1321 ± 113	182 ± 44	14 ± 5	25 ± 9	4 ± 6	4 ± 3
	6	923 ± 98	68 ± 19	4 ± 5	6 ± 4	4 ± 8	3 ± 4
	7	723 ± 36	48 ± 23	4 ± 4	4 ± 4	4 ± 6	4 ± 3

Table 3. Biomass burning events and mean enhancements in trace gases measured at Summit.

Event	Start Date	Event Length (h)	BC_{fire} (pmol mol^{-1})	ΔO_3[a] (nmol mol^{-1})	ΔPAN (pmol mol^{-1})	ΔNO_x (pmol mol^{-1})	ΔNO_y (pmol mol^{-1})	ΔC_2H_6 (pmol mol^{-1})	Plume age[b] (days)	Source[c]	BC_{anthro}[d]
1	25 Jul 2008	33	30.6	−4.6	6.3	5.7	12.6	48.6	9	NA	med
2	1 Aug 2008	15	25.0	7.0	–	1.8	20.9	–	15	NA	low
3	3 Aug 2008	252	90.7	10.5	83.5	13.9	141	–	14	NA	med
4	15 Mar 2009	60	58.6	−0.5	2.1	–	–	107	12	EU	med
5	18 Mar 2009	33	23.1	3.8	−1.1	–	–	−11.3	15	EU	med
6	21 Mar 2009	21	17.6	3.8	−20.9	–	–	11.6	16	EU	low
7	27 May 2009	30	17.7	10.7	71.6	–	–	–	16	AS	med
8	17 Jul 2009	12	19.9	4.6	67.2	6.2	108	−9.6	13	NA	low
9	18 Jul 2009	15	13.5	13.0	58.2	22.6	135	25.5	14	NA	low
10	16 Aug 2009	18	11.8	−4.1	3.3	16.0	11.8	–	18	NA	low
11	18 Aug 2009	12	9.5	5.7	74.4	7.5	65.4	113	17	NA	med
12	7 Jun 2010	27	11.3	8.9	–	5.6	105	13.1	13	NA	high
13	18 Jul 2010	51	27.4	4.3	–	4.7	97.3	27.8	9	NA	high

[a] Δ represents the enhancement over the background level (background = 20th percentile of each species for each month and year).
[b] Mean weighted age from FLEXPART.
[c] Primary BB source. NA = North America, EU = Europe, AS = Asia.
[d] Indicates potential contribution from anthropogenic pollution. Low: $BC_{anthro} < 50$th percentile, Med: BC_{anthro}, < 75th percentile, high: BC_{anthro}, > 75th percentile.

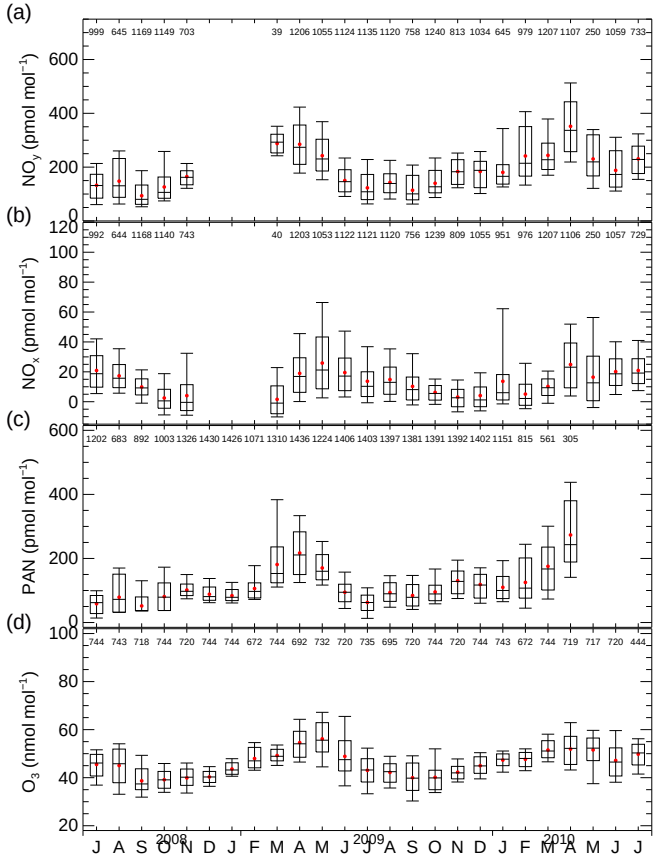

Figure 1. Monthly averages of **(a)** NO_x, **(b)** NO_y, **(c)** PAN, and **(d)** O_3 at Summit from July 2008–July 2010. The median and mean of the data are represented by a horizontal line and filled black circle, respectively; the box indicates the middle 67 % of the data; and the vertical whiskers indicate the 5^{th} and 95^{th} percentile of all the data. The numbers at the top of each plot represent the number of 30–min averages included in the distribution.

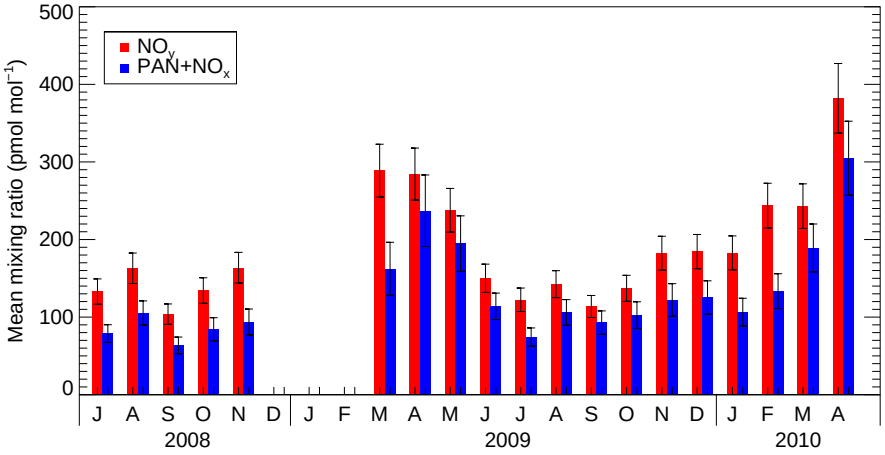

Figure 2. Monthly mean levels of NO_y and PAN+NO_x at Summit calculated from individual 30 min averages for 2008–2010 at Summit. Error bars represent uncertainty in the measurements resulting from measurement accuracy, calibration uncertainty, and artifact corrections as discussed in sections 2.2.1, 2.2.2, and the supplementary material. Uncertainties in PAN+NO_x were determined from the propagation of errors. Only coincident data are considered in this analysis.

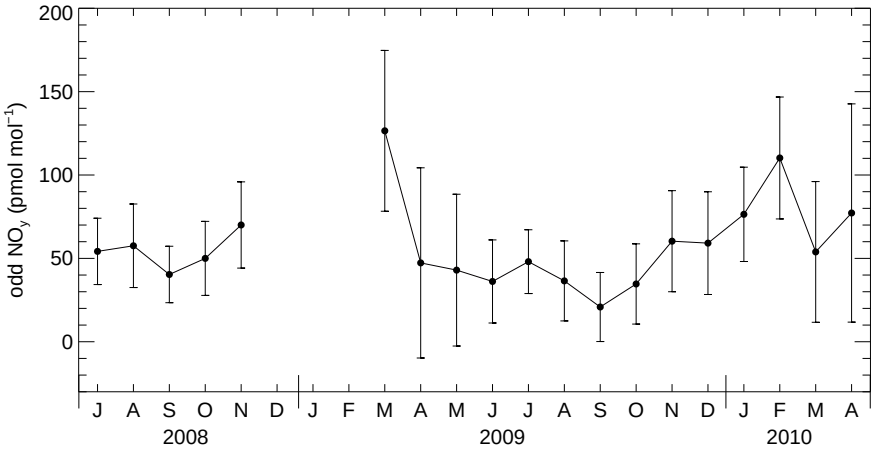

Figure 3. Monthly levels of odd NO_y (calculated from the 30 minute averaged NO_y, PAN, and NO_x measurements) at Summit. Error bars represent the uncertainty in odd NO_y mole fractions, determined from the propagation of errors from PAN, NO_x, and NO_y.

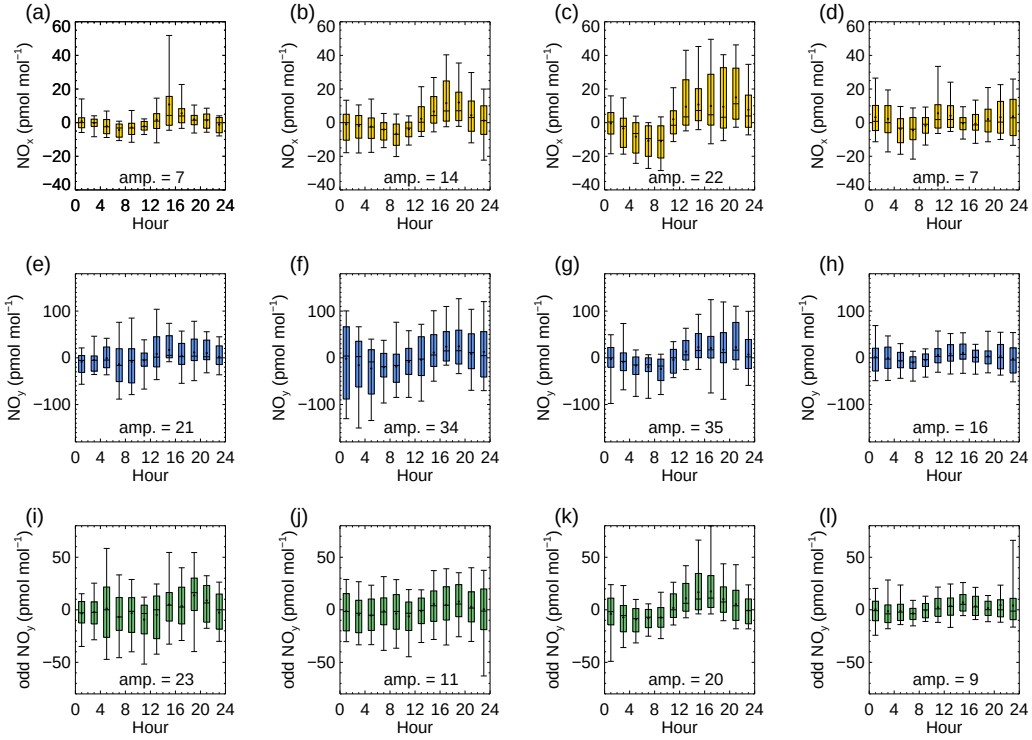

Figure 4. Average diurnal cycle of ambient NO_x **(a, b, c, d)**, NO_y **(e, f, g, h)**, and odd NO_y **(i, j, k, l)** measured at Summit for the months March (1st column), April (2nd column), May (3rd column) and, June (4th column) 2008–2010. Median ambient levels observed each day were subtracted, to remove any impact from day to day variability. The median and mean of the data are represented by a horizontal line, and filled black circle, respectively; the box indicates the middle 67 % of the data; and the vertical whiskers indicate the 5th and 95th percentile of all the data. Times are shown as local time (UTC).The amplitude of the diurnal cycle (given as the difference between the lowest and highest 2 hour median values, in $\mathrm{pmol\,mol^{-1}}$) is noted on each subplot.

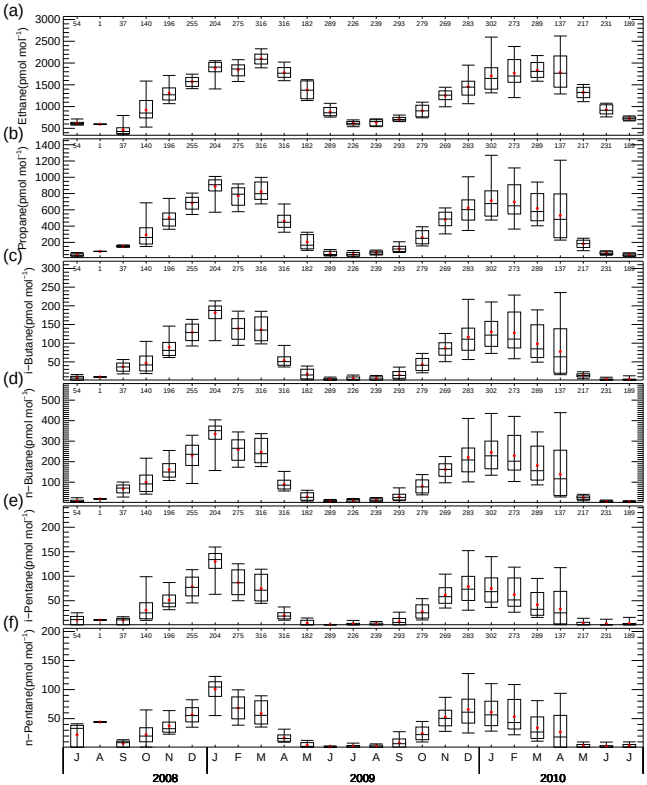

Figure 5. Monthly averages of **(a)** ethane, **(b)** propane, **(c)**, i-butane,**(d)** n-butane, **(e)** i-pentane, and **(f)** n-pentane, at Summit during from July 2008–July 2010. Median and mean are indicated by a horizontal line and black square, respectively; the box indicates the middle 67 % of the data; and the vertical whiskers indicate the 5th and 95th percentile of all the data. The numbers at the top of each plot represent the number of measurements included in the distribution.

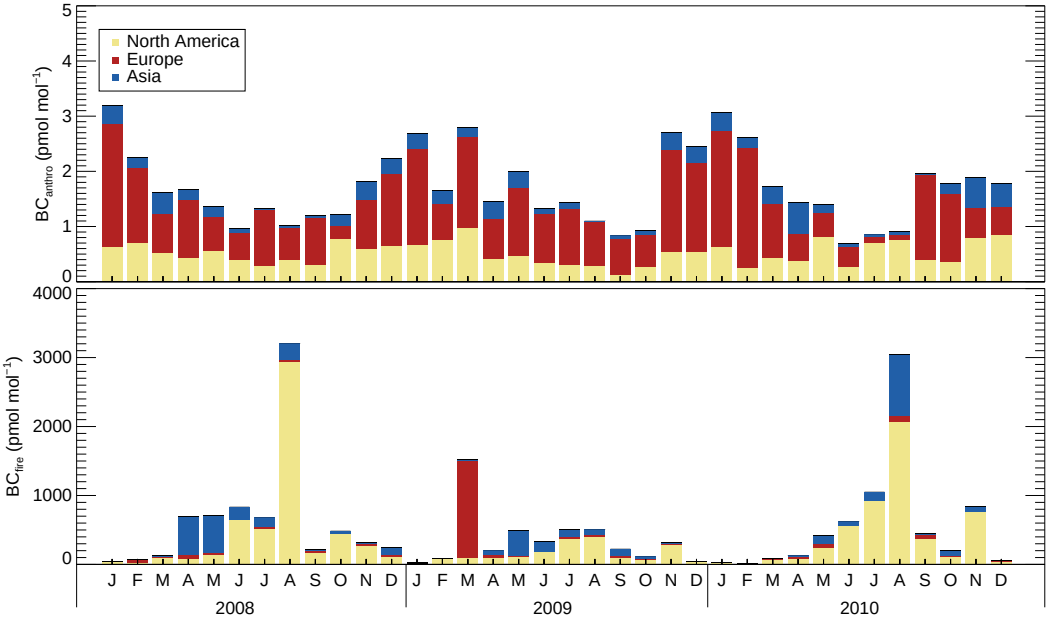

Figure 6. Barplot showing the total monthly BC_{anthro} (top) and BC_{fire} (bottom) tracer from FLEXPART for 2008, 2009, and 2010. The different colors represent the contributions from North America, Europe, and Asia as shown in the legend.

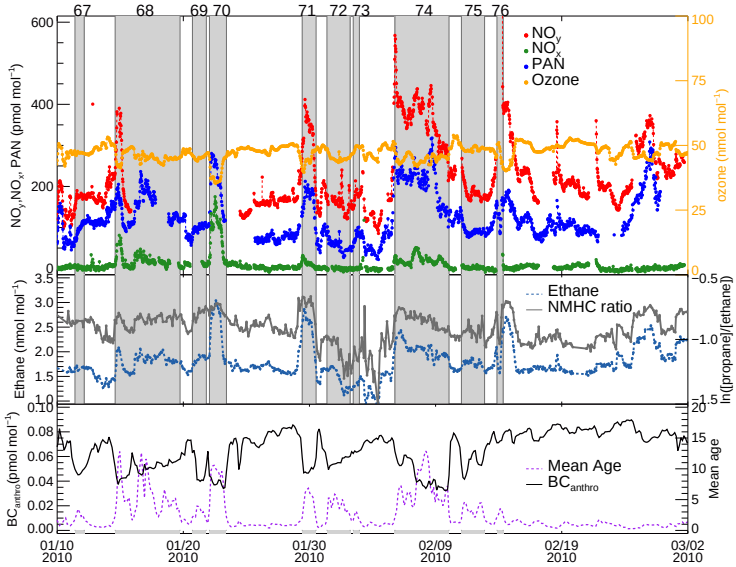

Figure 7. The top plot shows 30 min averages of NO_x, NO_y, PAN, and 1 h average of O_3 from Summit between January 10 and March 2, 2010. The middle plot shows ethane mole fraction and ln([propane]/[ethane]), and the bottom plot shows the FLEXPART BC_{anthro} tracer emissions (from all continents), and mean weighted age, for the same period. The shaded areas indicate the events discussed in detail in the main text and numbers at the top of the plot represent the event number (see supplementary material for details on the events).

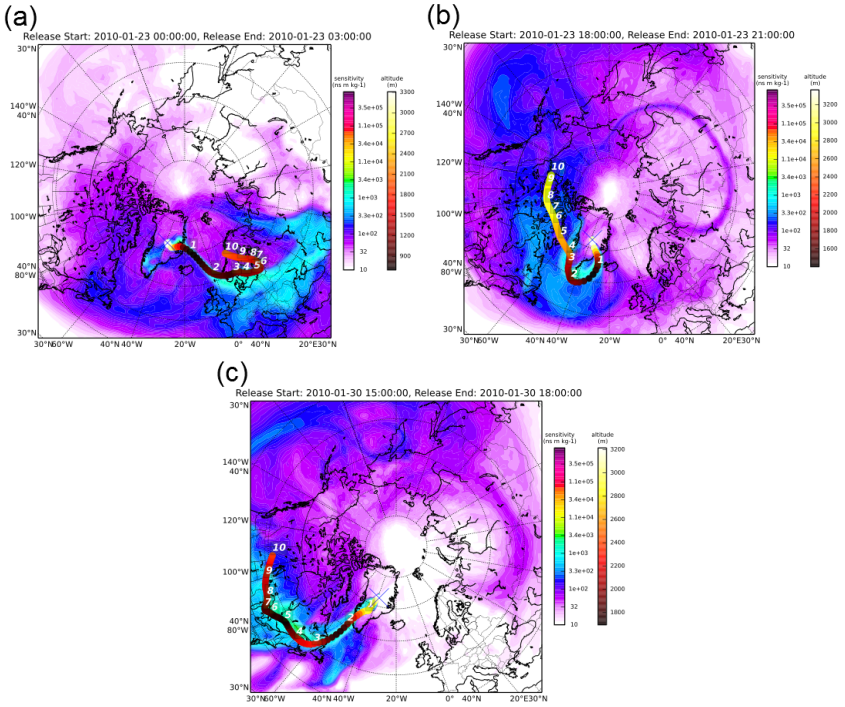

Figure 8. Simulated total column sensitivity (ns m kg^{-1}) for retroplumes originating at Summit on **(a)** 23 January, 2010, at 00:00 UTC, **(b)** 23 January, 2010, at 18:00 UTC, and **(c)** 30 January, 2010, at 15:00 UTC. The altitude circles represent the centroid location of the particles in the model domain N days back from the measurement date, where N is the number shown next to the shaded circles (up to 10 days are shown on the plots). The shading represents the altitude at three hourly intervals of the centroid location, given by the heat scale colorbar (note the change in scale for the colorbar).

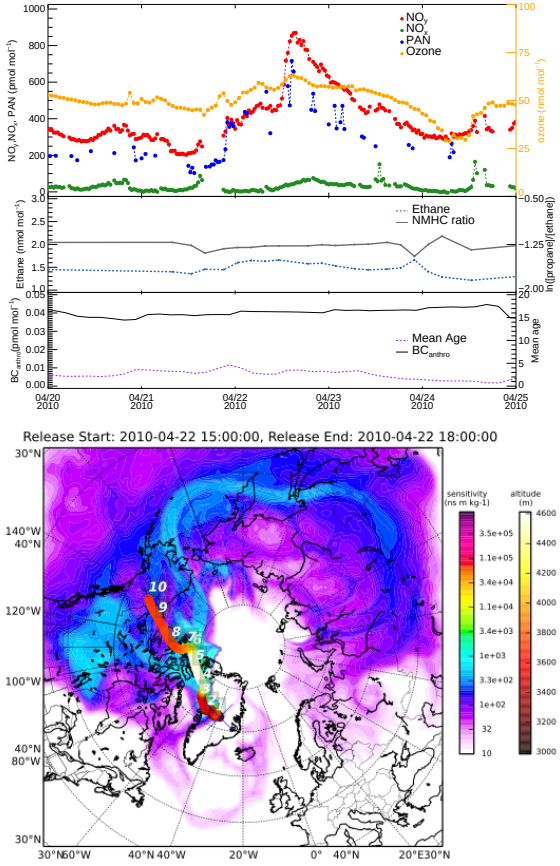

Figure 9. 30 min averages of NO_x, NO_y, PAN, 1 h average of O_3, C_2H_6, ln([propane]/[ethane], and FLEXPART BC_{fire} tracer and mean weighted age at Summit from 20-25 April, 2010. The vertical lines represent the arrival time of the FLEXPART simulated total column sensitivity at Summit on April 22, 2010, between 15:00-18:00 UTC, as shown in the bottom panel.

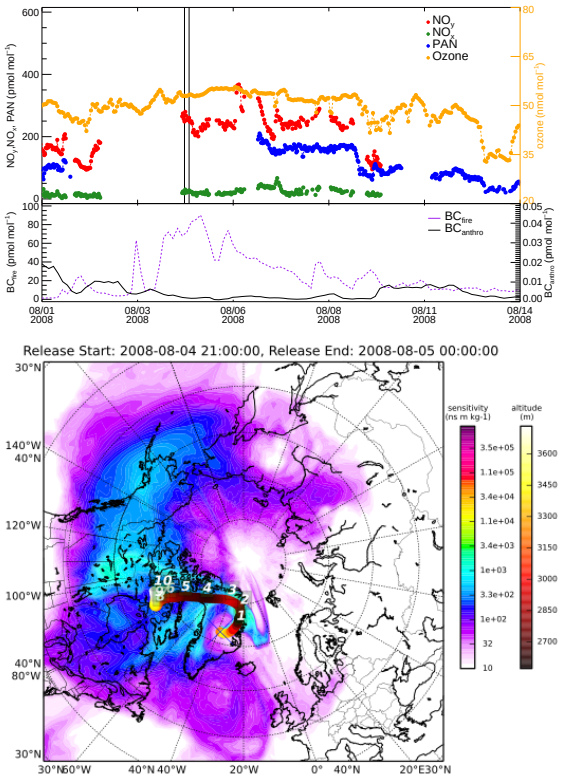

Figure 10. Top panel: 30 min averages of NO_x, NO_y, PAN, and 1 h average of O_3 and FLEXPART BC_{fire} and BC_{anthro} tracer at Summit from 1–14 August, 2008. The vertical lines represent the arrival time of the FLEXPART simulated total column sensitivity at Summit between 04 August, 2008, 21:00 UTC and 05 August, 2008, 00:00 UTC, as shown in the bottom panel.

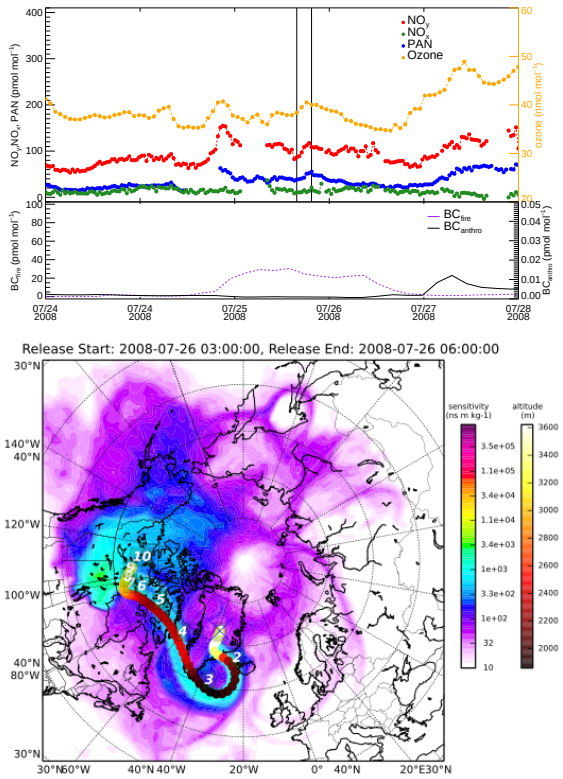

Figure 11. Top panel: 30 min averages of NO_x, NO_y, PAN, and 1 h average of O_3 and FLEXPART BC_{fire} and BC_{anthro} tracer at Summit from 24–27 July, 2008. The vertical lines represent the arrival time of the FLEXPART simulated total column sensitivity at Summit on 26 July, 2008, between 03:00-06:00 UTC, as shown in the bottom panel